Sunil Nautiyal*[1,2], Mrinalini Goswami[1], Satya Prakash[1], K.S. Rao[3,] R.K. Maikhuri[4], K. G. Saxena[5] , Sangeeta Baksi[6], Shravani Banerjee[1]

[1]Centre for Ecological Economics and Natural Resources (CEENR), Institute for Social and Economic Change (ISEC), Dr. VKRV Rao Road Nagarabhavi, 560072, Bangalore, India

[2]ZALF Fellow, Leibniz-Centre for Agricultural Landscape Research (ZALF), Eberswalder Str. 84, 15374 Muencheberg, Germany

[3]**Department of** Botany, University of Delhi, Delhi, 110007 India

[4]Department of Environmental Science, H.N.B. Garhwal University (A Central University), Uttarakhand 246174, India

[5]School of Environmental Science, Jawaharlal Nehru University, New Delhi 110067, New Delhi, India

[6] Technology Development Board, Department of Science & Technology, Block II, Second Floor, Technology Bhawan, New Mehrauli Road New *Delhi*-110016

*Corresponding Author: Sunil Nautiyal, Email: nautiyal_sunil@yahoo.com (https://orcid.org/0000-0002-1481-7754)

Spatio-temporal Variations of Geo-climatic Environment in a High-Altitude Landscape of Central Himalaya: An Assessment from the Perspective of Vulnerability of Glacial Lakes

Abstract

Impacts of climate change on snow cover, permafrost and glaciers at varied elevations are wide ranging and well-known. Melting water from glaciers forms glacial lakes; where, under the changing climate and accelerating glacial retreats have been a prime cause of glacial lake growth and outbursts. Indian Himalayan Region has also witnessed those impacts on glacial lakes with several evidences of glacial lake outbursts in recent years affecting people and ecosystems. Thus, to provide an understanding of geoclimatic environment and glacial lakes of the region, this article has attempted to look into the spatio-temporal changes of climatic conditions and physical landscape in Chamoli district of Uttarakhand in Indian Himalayan Region. In this study, mapping of glacial lakes in the district has been done to look into the aspects of associated hazards. The assessment has been done using historical trend analysis of climatic parameters, land surface temperature and physical landscape change in the study area. Seismic activities of the region have also been taken into account to understand the vulnerability of glacial lakes. The results indicate dynamic environmental conditions with visible physical landscape change; where, increase in built-up area by 541.57 Km^2, decrease in dense forest and fallow land by 76.96 Km^2 and 364.09Km^2 respectively over a period of two decades (2000-2020) have been observed. Minimum temperature has been gradually increasing by 0.68°C per decade. The geospatial analysis provides identification of ~500 glacial lakes, where 40.92% are situated at 5000-6000 m elevation. It is understood that glacial lakes of the study area are prone to produce disasters in the region because of changing climate and active seismicity, and lakes at higher elevation are highly susceptible to GLOF (Glacial Lakes Outburst Flood). Moreover, prevalence of large number of supraglacial lakes in the study region which are dynamic in nature, makes the area more vulnerable to hazards. The very old supraglacial lakes in high altitude region need attention and detailed study in terms of their changing characteristics and stability. Anthropogenic interventions in the area are contributing towards higher intensity of impacts on human and resources. It is suggestive that further development activities should consider the potential hazards and vulnerable zones in study area for disaster risk reduction.

Keywords: GLOFs; Indian Himalayan Region, Climate Change; High Altitude Lakes

Introduction

Landscape change and climate change are of global concerns and associated in a feedback loop. The change in landscape due to the impacts of climate change has widely reported by the scientific community. Recent research revealed that change in landscape is mostly due to the rapid urbanization which has negatively affected the land surface temperature (Yuen and Kong, 2009; Fonseka et al., 2019; Arulbalaji et al., 2020; Das et al., 2020). Increase in urbanization is leading towards change in land use land cover pattern and creates environmental as well as climatic disturbances (Xiao et al., 2006). Physical landscape change has impacts on land surface temperature (earth surface temperature) (Kafy et al., 2020; Zhang and Sun, 2019); which is the soil surface temperature for bare soil and canopy surface temperature for vegetation. The radiating temperature of the earth's surface that controls surface heat and water exchange by the atmosphere represents land surface temperature (Yuan and Bauer, 2007).

According to United Nations' World Urbanization Prospects (2019), 55% of the world population lived in urban areas that is expected to increase by 68% by 2050. In 1950, the global urban area was only 3% that is expected to increase by 66% in 2050 (United Nations, 2018). Rapid urbanization has been considered as important drivers of loss of biodiversity, climate change, vegetation and agricultural loss and various other environmental issues (McCarthy et al., 2010; Chen et al., 2006). The impacts include replacement of vegetation with built-up areas resulting in increase of land surface temperature by trapping more solar radiation on earth's surface. Impervious surface with less vegetation cover has low albedo and positive relationship with land surface temperature. Spatial and temporal analysis of urban growth is important to understand the urban climate studies, future sustainable planning and development (Dadras et al., 2015). Land surface temperature (LST) varies in response to the surface energy balance and modulates the air temperature of the lowest layers of the urban atmosphere, which is central to the energy balance of the surface and affects the energy exchanges that may disturb the comfort of the people dwelling in that area (Voogt and Oke, 2003). There are some studies which illustrates the relationship between LST and air temperature (Hachem et al., 2012; Urban et al., 2013; Vancutsem et al., 2010). LST and air temperature are closely associated with the vegetation surfaces since under cloud cover the insolation is low and LST and air temperature may fluctuate by 1-2^{O}C (Good et al., 2017). The difference between LST-T2m temperatures may approach or even exceed 20°C during the middle of the day in clear sky in low latitudes over non-vegetation areas (Good et al.,

2016; Mildrexler et al., 2011). Monitoring of high resolution satellite images has made it possible to understand the effects of urbanization on land surface temperature with the help of thermal images by single infrared channel method or the split window method (Pu et al., 2006; Streutker, 2002). The satellite temperature measurements provides more accurate results than the in-situ measurements (Cheval and Dumitrescu, 2009). The amalgamation of remote sensing and GIS are widely used to understand spatial temporal variation over the land surface. Multi-spectral Landsat and Sentinel satellite data are extensively used to understand the land use land cover change dynamics as well as the land surface temperature where the inclusion of thermal bands have made it suitable (Hu and Jia, 2010; Keshtkar and Voigt, 2016). In previous studies, researchers have used satellite images to understand the land surface temperature and its various key factors to assess the linkages with health related issues and heat related risks (Running et al., 1994; Crago et al., 1995; Kimura and Shimiru, 1994; Weng and Fu, 2014; Hu and Brunsell, 2013; Deng and Wu, 2013; Mathew et al., 2016).

Himalayan regions are fragile eco-environments that play an important role in maintaining the ecosystem services and natural resources. Himalayan environments are highly sensitive towards environmental pressure and climate change whereas any jeopardy in that environment will further intensify global environmental concerns. However, the Himalayan region is affected by global warming, anthropogenic activities such as urbanization and exploitation of resources that result in a rapid retreat of glaciers in this eco-sensitive zone (Khadka et al., 2018). Climate change has always been a concerned research for Himalayan region (Shrestha et al., 1999, Liu and Chen, 2000). There are reports and studies available that show the increasing instances of glacial retreat, snow melt and permafrost degradation as well as significant changes in hydrology and water resources (Kang et al., 2010, Yao et al., 2012a, Yao et al., 2012b). The studies focusing on Western Himalayan region revealed a warming rate of 0.16^{o}C annual mean temperature per decade during 1955-1996 (Liu and Chen 2000). In the last century, a significant increase in winter and annual temperature was observed over Western Himalayas (Mann et al., 1999, Kothawale and Kumar, 2005, Bhutiyani et al., 2007). Winter season temperature in Himalayan region has experienced significant rise which is a matter of concern (Bhutiyani et al., 2007, Shrestha et al., 2010, Dimri and Dash, 2012). Increase in temperature leads to various consequences in Himalayan region such as rapid growth of tree rings in higher altitudes (Borgaonkar et al., 2009). Climate change in Himalayan region can also be attributed to blooming tourism activities that has led to

infrastructure development to achieve good economic benefits (Wang and Zhou, 2019). Glacier regions are always highly sensitive to climate change; where, the increase in temperature directly leads to melting of glacier (Chevallier et al., 2011, Haeberli et al., 2013, Mool et al., 2011). Melting of glacier results in the formation of supraglacial lakes that coalesce to produce proglacial lakes. Most of the proglacial lakes are moraine-stricken, which can lead to a rapid release of the water and sediment, often called Glacial Lake Outburst Floods (GLOFs), (Maskey et al., 2020).

The Indian Himalayan Region (IHR) has been facing a wide range of challenges in dealing with the adverse effects of climate change. The IHR is always affected by different glacier related disasters; recently on 7 February 2021, Uttarakhand has faced glacier burst resulting in sudden overflow in Dhauli Ganga, Rishi Ganga and Alaknanda rivers and their tributaries. The event triggered widespread panic and large-scale devastation in the high mountain areas (see annesure). NTPC's Tapovan Vishnugad hydel project site and Rishi Ganga Hydel project site have undergone massive damage and nearly hundred people lost their lives. In another such episode in 2013, Uttarakhand Kedarnath region faced flash floods where 6000 people lost their lives.

Climate change, particularly increase in temperature, has been a concern in glacial regions. The adverse effects to mention include occurrence of more severe GLOFs, increase in frequency of GLOFs, shrinkage of glaciers and increase in glacial lakes (Reynolds, 1992; Clague and Evans, 1993; Walder and Driedger, 1995; Rai, 2005). GLOFs may endanger the lives, infrastructure and result in flash floods (Walder and Costa, 1996; Rudoy, 2002; Liu et al., 2013). Lu and Li (1989) reported that humidity and dry heat are responsible for outburst in Tibet. Chen et al. (2010) has found that increase in temperature is responsible for the increase in frequency of GLOF in Yarkant region of Karakoram. The intensification of glaciological hazards in IHR is evident with adverse consequences where the recent disaster in Chamoli district has attracted much attention. Therefore, we considered to analyse the air temperature, land surface temperature, and land use land cover change to understand different aspects of changing climatic conditions and probable factors associated with glacier burst and its consequences in Chamoli district. This paper has also intended to understand landscape change, land surface temperature, different aspects of glacier bursts and dynamics of glacial lakes.

Study Area:

The Chamoli district lies in the central Himalaya and surrounded by Uttarkashi in north-west, Rudraprayag in west, Pithorgarh and Bageshwar in east and Almora in south (Figure-1). Geographically, the district is bounded by latitude N 29^0 15'00" and $31^0$00'00" and longitude E $79^0$15'00" and $80^0$00'00", covering geographical area of 7604 sq.km. The district is divided into 10 tehsils namely Joshimath, Chamoli, Karnaprayag, pokhari, Garsain, Tharali, Narayanbagar, Jilasu , Adibadri and Ghat. As per the census 2011, the total population of Chamoli district is 391605 (Census, 2011).

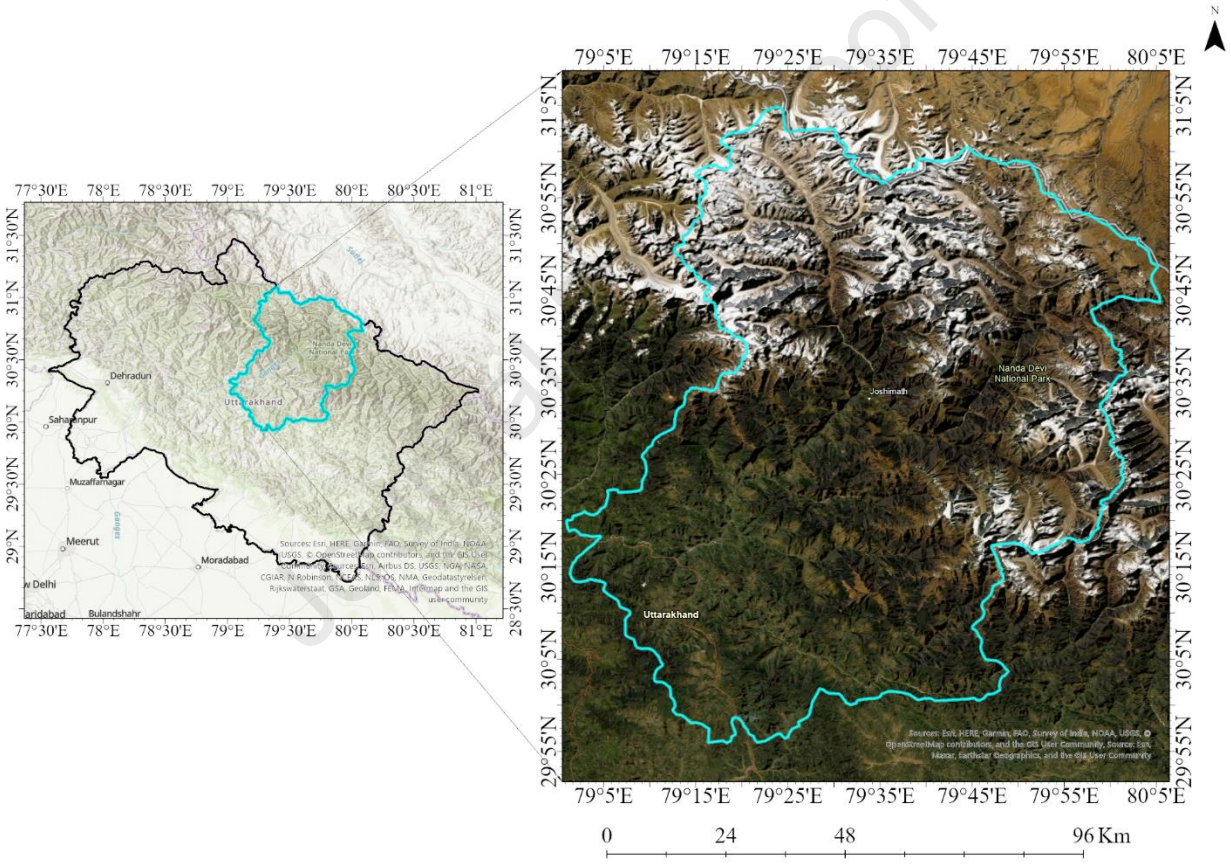

Figure 1: Study area map of the Chamoli district, Karnataka, India

The district represents many distinct ecological and geographical features. The major drainage of the Chamoli district is Alaknanda and its tributaries Dhauli Ganga, Nandakini, Pindar, Birhi ganga etc. Chamoli district is surrounded by hills and mountains with very narrow valleys, deep gorges. Physiographically, the catchment of Alaknanda River belongs to Gangotri -Badrinath-Kedarnath river system. The hilly slopes are covered with glaciers. The prevalent landforms of Chamoli

district are U-shaped glacier valleys, V-shaped fluvial valleys, lateral moraines, end moraines, river terraces and denudational structural mountain. The soils of Chamoli district are natural, dynamic and heterogeneous. The rocks such as granite, shale, gneiss, phyllite, shale, slate, etc. developed into soils under cool and moist climatic conditions. The maximum and minimum temperature ranges from 31 to -2.9^{o}C. The rainfall varies with respect to altitudes and the average rainfall is 1230.8 mm.

Data used:

Data used in the study for geospatial analysis are presented in table-1. Landsat satellite imagery is used to monitor and analyze Land Surface Temperature (LST) and Land Use Land Cover (LULCC) in the present study. Evaluation of spatio-temporal analysis of LST and LULCC were taken for two decades-2000, 2008, 2013 and 2020. The data is obtained from US Geological Survey (USGS).

Table 1: Data used in the present study

Satellite Sensor/Data	Year	Resolution	Source
Landsat 4/5 TM	2000	30 m	USGS (https://earthexplorer.usgs.gov/)
Landsat 4/5 TM	2008	30 m	USGS (https://earthexplorer.usgs.gov/)
Landsat OLI/TIRS	2013	30 m	USGS (https://earthexplorer.usgs.gov/)
Landsat OLI/TIRS	2020	30 m	USGS (https://earthexplorer.usgs.gov/)
Sentinel 2A	2020	10 m	European Space Agency (https://sentinels.copernicus.eu/web/sentinel/home)
Seismological Data	2000-2021	-	National Center for Seismology (https://seismo.gov.in/)

Maximum temperature, minimum temperature and relative humidity data for variability and trend analysis have been obtained from NASA POWER (https://power.larc.nasa.gov/data-access-viewer/). The metrological data has been based on Modern Era Retrospective-Analysis for Research and Applications (MERRA-2) assimilation model. Gridded daily Temperature at 2 Meters, Maximum Temperature at 2 Meters and Minimum temperature with 0.5*0.5 resolution from 1982 to 2020 was obtained and used for trend analysis.

Methodology

Meteorological data:

Maximum and minimum temperature and relative humidity were used to analyze the variability and trend analysis in Chamoli district. Trend detection and analysis are performed through parametric and non-parametric tests only for consistent data. The non-parametric statistical test has an advantage over the parametric test in that it is better suited to non-normally distributed, outlier, censored, and missing data, which are common in hydrological time series. Therefore Mann-Kendall (MK) test in used to analyze the trend of all metrological parameters (Degefu and Bewket, 2014; Seleshi and Zanke, 2004, Tabari *et al.*, 2015). The MK test is a non-parametric test that examines a time series for a trend without determining whether the trend is linear or non-linear (Yue et al., 2002).

Land use Land cover change:

As per the availability of satellite imagery, Landsat4-5 TM and Sentinel 2A data were used for the mapping of land use land cover classification. All the bands of both satellite imagery were stacked and generated a False Color Composite (FCC) in QGIS software. To prepare the land use land cover map of Chamoli district from satellite imageries, supervised classification techniques were used to extract the feature classes. Nine major LULC classes were selected to map the Chamoli district viz; Barren land, Dense Forest, built-up, water bodies, fallow land, vegetation, snow/glacier, other features and shadow. Maximum likelihood classification scheme was adopted to classify the features. Before the selection of training samples, empirical analysis of satellite imagery with google earth images and toposheet were investigated carefully. Several training samples were taken for define each feature class. LULC map of 2000 was created using Landsat imagery and LULC map of 2020 was created using sentinel imagery. The change in land use land cover from 2000 to 2020 were extracted to conduct further analysis.

Glacial lakes inventory:

Inventory of different types of glacial lakes have been done based on visual interpretation and analysis of Landsat satellite imagery and Google Earth engine for the year 2019. The elevation of each glacial lakes has been extracted using ASTER Global DEM (Digital Elevation model) data. Moreover, area and volume of glacial lakes has been calculated to understand the dynamics of the

188 glacial lakes in the study area. Furthermore, Glacier inventory data has been collected from
189 Randolph Glacier Inventory to understand the association of glaciers with glacial lakes.

190 Volume of lake water estimation has been done for three randomly selected lakes to understand
191 the change in lakes' characteristics from 2000 to 2022. The volume of lake has been estimated
192 using the equation (Cook and Quincey, 2015):

193 $$V = 2 \times 10^{-7} A^{1.3719} \quad (1)$$

194 Whereas V= Volume of the lake (in $m^3 x10^6$) and A is the area (in m^2)

195 ***Retrieval of Land Surface Temperature from Landsat-5 TM:***

196 Evaluation of LST was based on the methodology of Chen et al. (2002); primarily for the
197 estimation of brightness temperature from Landsat-5 TM satellite imagery- the digital numbers
198 (DNs) of band 6 were converted into radiation luminance (RTM6) using the algorithm-

199 $$R_{TM6} = \frac{V}{255}\,(R_{max} - R_{min}) + R_{min} \quad (2)$$

200 V is DN of band 6,

201 $$R_{max} = 1.896(mW * cm^{-2} * sr^{-1}) \quad (3)$$

202 $$R_{min} = 0.1534(mW - cm^{-2} * sr^{-1}) \quad (4)$$

203 Further the radiation luminance was converted into satellite brightness temperature (BT) in
204 degree Celsius (^{0}C) using algorithm-

205 $$BT = \frac{K1}{(\ln\left(\frac{K2}{\frac{R_{Tm6}}{b}}+1\right))} - 273.15 \quad (5)$$

206 K1 = 1260.56 K and K2 = 607.66 (mW * cm^{-2}*$sr^{-1}$$\mu m^{-1}$), are calibration constants under an
207 assumption of unity emissivity; where b represents the effective spectral range when the sensor's
208 response in considerably higher than 50%, b=1.239 (μm) (29).

209 *Retrieval of Land Surface Temperature from Landsat-8 OLI/TIRS:*

For the retrieval of LST from Landsat-8 satellite imagery, primarily the DN of thermal infrared band was converted into spectral radiance(L_λ) by using the algorithm from Landsat user's handbook (2016):

$$L_\lambda = M_{LQcal} + A_L \quad (6)$$

L_λ is TOA spectral radiation in watts/ (m^2 * ster * µm), M_L is band specific multiplicative rescaling factor from metadata, A_L is band specific additive rescaling factor, and Qcal is symbolized values of quantized and calibrated standard product pixels (D).

Then band radiance is converted into BT in degree Celsius (^{0}C) using algorithm-

$$BT = \frac{K2}{\ln(\frac{K1}{L_\lambda}+1)} - 273.15 \quad (7)$$

BT- Brightness temperature in Celsius and K1 and K2 are thermal conversion from metadata.

Surface Emissivity (ε) Retrieval: The algorithm used for the land surface emissivity (ε) values are

$$\varepsilon = m \,.\, PV + n \quad (8)$$

where m = 0.004 and n = 0.986. PV is proportion of vegetation extracted from algorithm

$$PV = \left(\frac{NDVI - NDVI_{min}}{NDVI_{max} - NDVI_{min}}\right)^2 \quad (9)$$

$$NDVI = \left[\frac{NIR - RED}{NIR + RED}\right] \quad (10)$$

Where NDVI represents the normalized difference vegetation index. NDVI index describes the vegetation cover of the earth that can be estimated using the visible and near-infrared reflectance. $NDVI_{min}$ represents the minimum value of NDVI and $NDVI_{max}$ represents the maximum value of NDVI.

Further the LST was estimated with the help of emissivity corrected LST values.

However, brightness temperature (BT) represents the temperature of blackbody which would emit the same amount of radiation as the target body in a specified spectral band. Since, the BT assume as blackbody, which it is not and this can cause errors in surface temperature. Hence emissivity correction is evaluated to produce the LST from BT while minimize the errors: -

$$LST = \frac{BT}{1+(\lambda(BT)*\frac{\ln(\varepsilon)}{\rho})} \quad (11)$$

LST is in degree Celsius, BT is brightness temperature in Celsius, λ is the wavelength of emitted radiation, ρ = h*c/σ = 1.438 * 10^{-2}mK, σ is Stefan-Boltzmann constant, h represents Planck's constant, c represents velocity of light and ε represents land surface emissivity (LSE).

Furthermore, the relative changes of LST were extracted to analyze the major change in Chamoli district from 2000 to 2020 using equation: -

$$\text{Relative Change of LST} = \frac{(LST\ of\ 2020 - LST\ of\ 2000)}{LST\ of\ 2000} * 100 \quad (12)$$

Results and Discussion

Meteorological Analysis

Temperature

Temperature rise is the top amongst all the global climate change manifestations. For the years 1982–2020, annual and monthly temperature data were analyzed to determine the variability and trend of temperature change in the study area. The monthly and annual temperature trend is presented in Table-2. The mean temperature in this district ranges from -2.51 ^{o}C minimum to 19.52° C maximum with annual average temperature of 6.57^{o} C. The rate of change in minimum temperature per decade is 0.68°C with visible gradual increase; whereas the maximum temperature has been decreased by 0.59^{o}C per decade from 1982 to 2020. The long-range anomalies of mean annual temperature showed inter-annual variability while the fluctuation of trend is very high and increasing trend after 1997 has been higher than the previous period. Maximum temperature is higher in 1984 to 1985 followed by a meagre decrease in later years as shown in figures- 2&3; whereas the minimum temperature is constantly rising from 1994 to 2020 as shown in figures- 2&4.

Table 2: MK trend test of Maximum and Minimum Temperature

Month	Mean	TMax			TMin		
		Z Value	Sen's Slope	P-value	Z Value	Sen's Slope	P-value
Jan	-2.72	-0.4597	-0.0119	0.6457	0.6897	0.0130	0.4904
Feb	-1.64	0.5807	0.0143	0.5615	0.9921	0.0315	0.3212
Mar	2.29	-0.4839	-0.0109	0.6285	0.0968	0.0021	0.9229
Apr	7.22	-0.4839	-0.0180	0.6285	2.2262	0.0403	0.0260

May	10.98	-1.8145	-0.0443	0.0696	2.6133	0.0410	0.0090
Jun	13.60	-2.7581	-0.0479	0.0058	2.6379	0.0317	0.0083
Jul	14.20	-2.9274	-0.0336	0.0034	3.4367	0.0271	0.0006
Aug	13.49	-2.1049	-0.0209	0.0353	2.9283	0.0200	0.0034
Sep	11.27	-0.2177	-0.0023	0.8276	2.4809	0.0341	0.0131
Oct	6.89	-0.6532	-0.0108	0.5136	3.3269	0.0448	0.0009
Nov	3.32	0.2177	0.0011	0.8276	3.0858	0.0379	0.0020
Dec	-0.06	0.2177	0.0011	0.8276	-0.3145	-0.0037	0.7531
Annual	6.57	-1.7903	-0.01866702	0.0734	3.3145	0.025942	0.00092

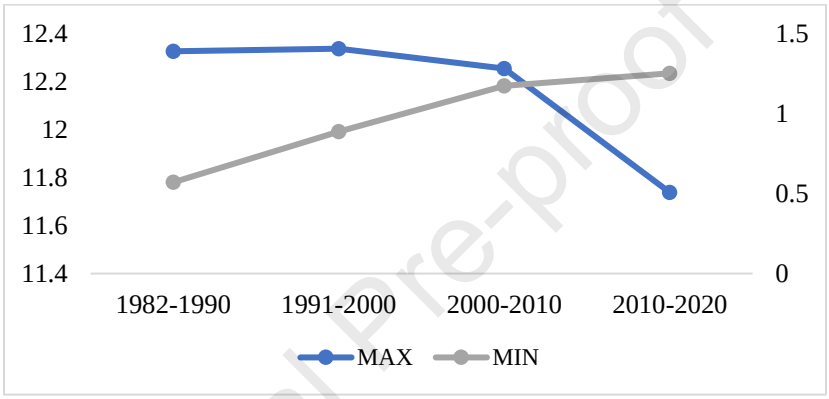

Figure 2: Decadal change in Maximum and Minimum temperature

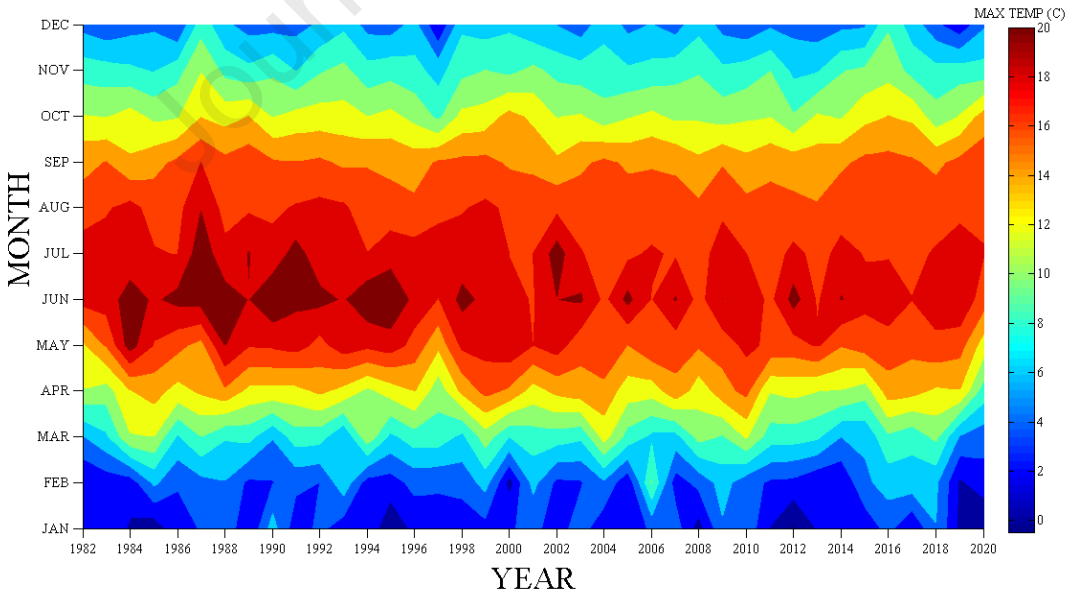

Figure 3: Maximum temperature of the Chamoli district from 1982-2020

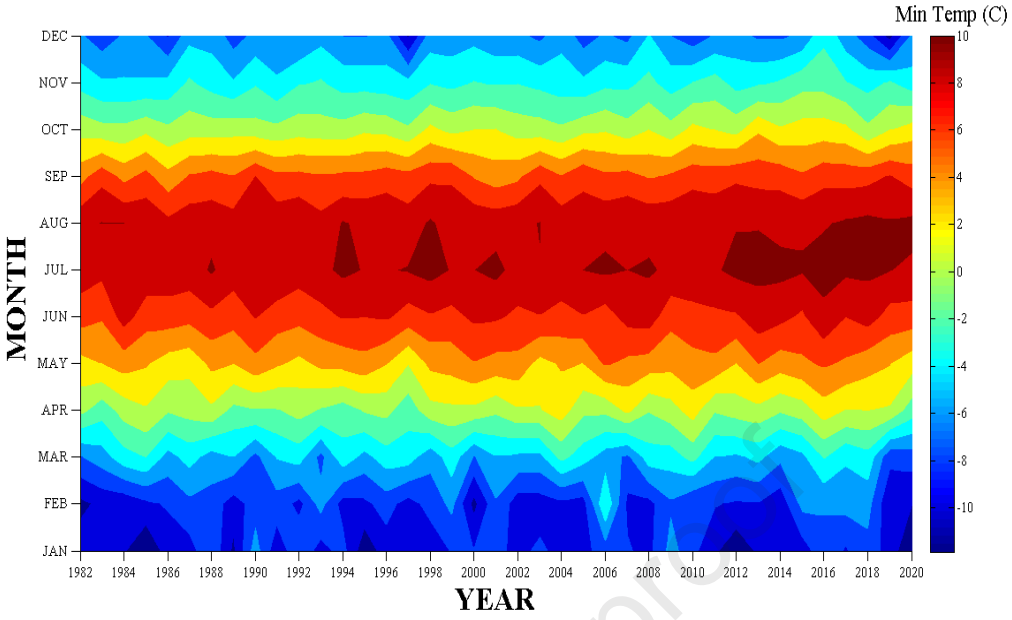

Figure 4: Minimum temperature of the Chamoli district from 1982-2020

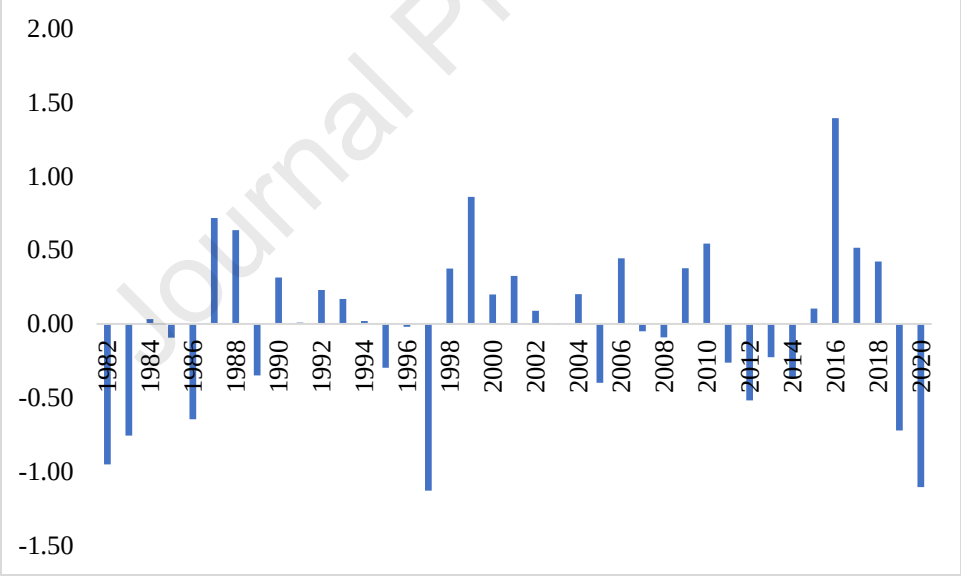

Figure 5: Temperature Anomalies of the Chamoli district

Further, monthly and annual average, maximum and minimum temperature trends have been analyzed using MK trend test and Sen's slope at 95% confidence level. Temperature anomalies of the district over the study period is presented in Figure-5. The trend for monthly maximum temperature showed a non-significant decreasing trend (except for the months of June, July and August) while a significant increasing trend for minimum monthly temperature was obtained for

all months (except for December). The overall annual temperature observed in the study area is attributed to an increase in minimum temperature. The increase of minimum temperature is more pronounced than any change in maximum temperature over the studied years.

Relative Humidity

Table 3: MK Trend test of Relative Humidity from 1982-2020

Month	Z value	Sen's Slope	P-Value
Jan	2.0807	0.4117	0.0374600
Feb	1.9719	0.3863	0.0486200
Mar	1.8629	0.3843	0.0624700
Apr	2.7704	0.4214	0.0055990
May	3.0607	0.4375	0.0022080
Jun	2.8672	0.4586	0.0041420
Jul	4.1613	0.3229	0.0000316
Aug	3.7866	0.1958	0.0001527
Sep	2.4678	0.2117	0.0136000
Oct	3.2543	0.3982	0.0011370
Nov	4.0162	0.4548	0.0000592
Dec	1.5000	0.1867	0.1336000
Annual	4.9113	0.3703	0.0000009

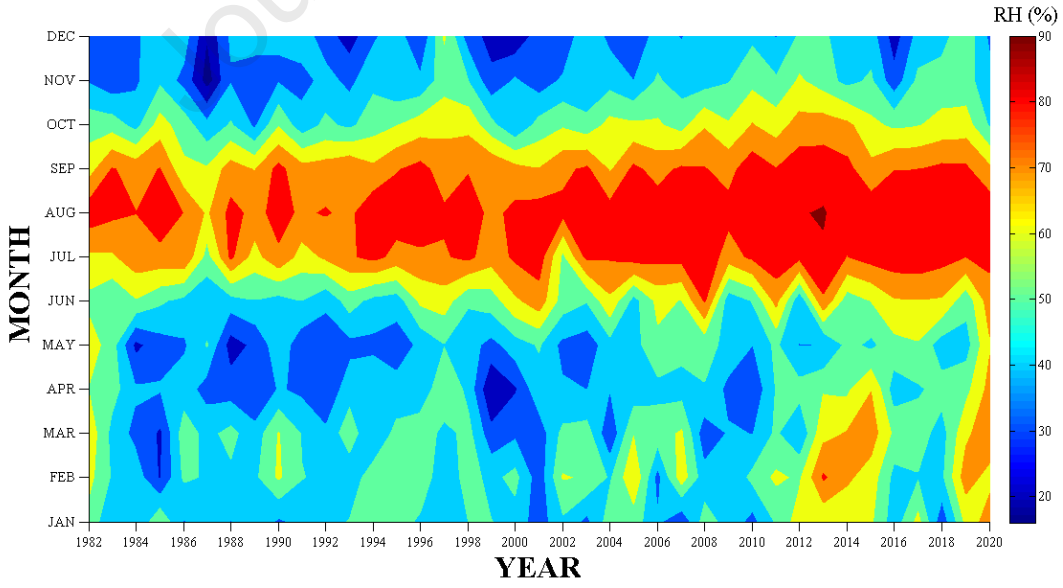

Figure 6: Relative Humidity of the Chamoli district from 1982-2020

An increase in humidity which represents the good amount of moisture availability in study area has been observed. The relative humidity has been constantly high or increased in the month of July, August and September after 2010 (Figure-6). Before 2010, the relative humidity is fluctuating over the studied time period. The MK monthly trend report shows a significant increasing trend for relative humidity for all months; whereas May, July, August and September months are with highest z values (Table-3). Increase in Z value represents the highest increment of relative humidity.

Land Surface Temperature

Land surface temperature was analyzed for 2000, 2008, 2013 and 2020 for Chamoli district. Estimated LST profile of the study area indicates that the temperature is fluctuating very high in this district whereas maximum LST is continuously increasing. Maximum LST was 33.66 ^{0}C in year 2000 then 35.65^{0}C in 2008, where the maximum temperature was increased by 1.99^{0}C from 2000 to 2008. Further, the maximum temperature was decreased by 4.04 ^{0}C from 2008 to 2013. Again, the temperature was increased by 5.08 ^{0}C from 2013 to 2020. Overall, the maximum temperature was increased by 3.03 ^{0}C from 2000 to 2020. The minimum temperature was increased by 10.53 ^{0}C from 2000 to 2020.

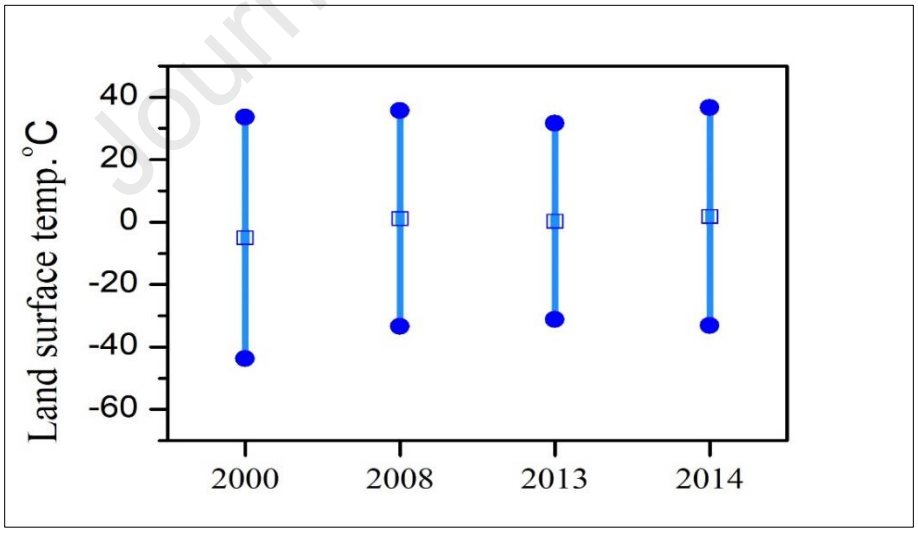

299 **Figure 7: Maximum and Minimum land surface temperature of the Chamoli district**

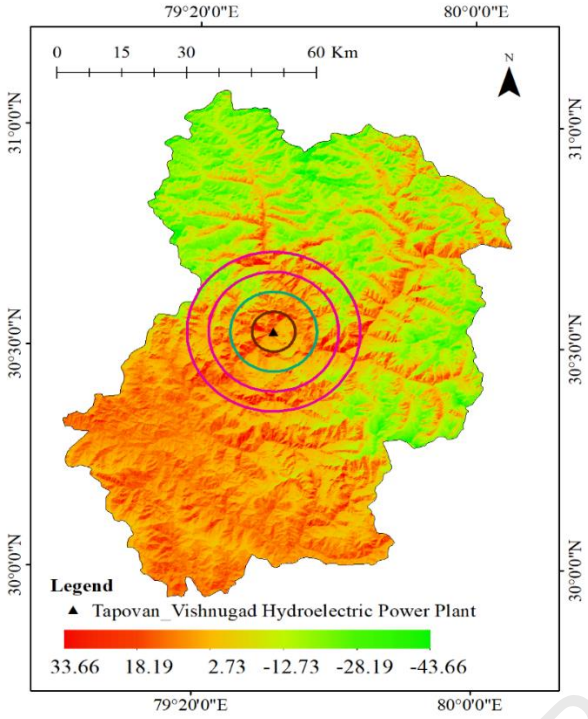

300

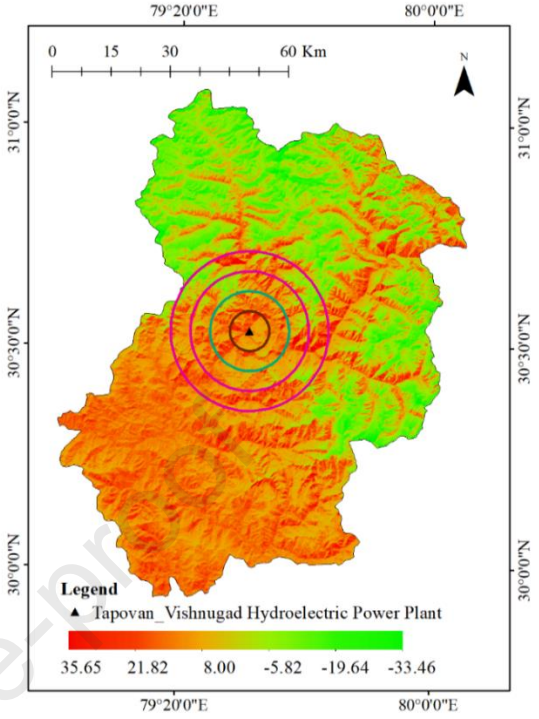

301 **Figure 8: LST of Chamoli district year 2000** **Figure 9: LST of Chamoli district year2008**

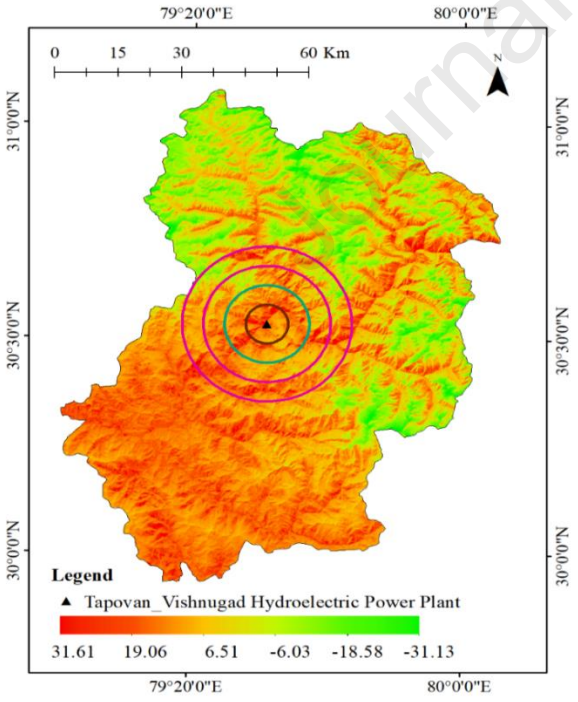

302

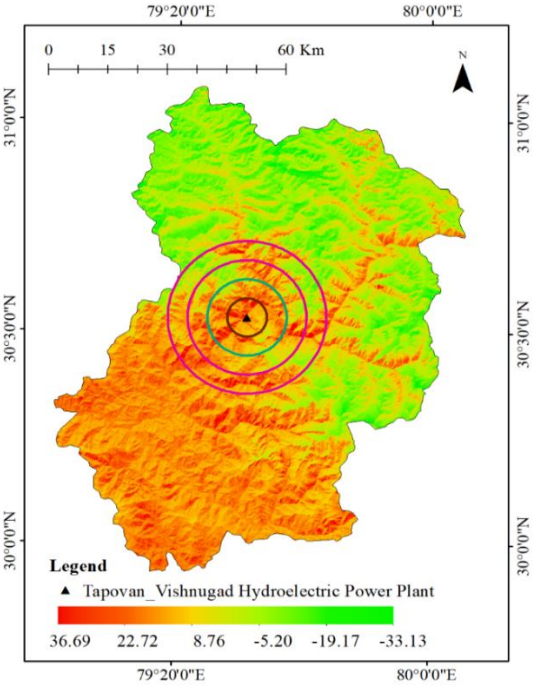

303 **Figure 10: LST of Chamoli district year 2013** **Figure 11: LST of Chamoli district year 2020**

The major findings of the LST analysis were represented through temperature profile in and around Tapovan-Vishnugad Hydroelectric Power Plant (Table-4). The buffer distance of 5 km were created to analyse LST from Tapovan-Vishnugad Hydroelectric Power Plant (Figures- 8,9,10, &11). Maximum LST in all buffer zone results indicate that A is 31.65 ^{0}C in 2000 and 28.35^{0}C in 2008 whereas it increases up to 28.78^{0}C in 2013 and 27.49^{0}C in 2020, B is 31.65 ^{0}C in 2000 and 34.46 ^{0}C in 2008 whereas its decreases in 2013 i.e., 28.89^{0}C and increases in 2020 i.e., 30.88^{0}C, C is 30.83^{0}C in 2000 and 34.46^{0}C in 2008 whereas its decreases in 2013 i.e., 29.73^{0}C and increases in 2020. D is 31.65^{0}C in 2000 and 32.05^{0}C in 2008 whereas its decreases in 2013 i.e., 28.95^{0}C and huge increase in 2020 i.e., 35.69^{0}C. Whereas, minimum land surface temperature results indicate that A is -4.04^{0}C in 2000 and 1.37^{0}C in 2008 then sudden increase in 2013 i.e., 3.95^{0}C and decrease in 2020 i.e., -5.87^{0}C. B is about -18.45^{0}C in 2000 and its increases in 2020 i.e, -16.58^{0}C. C is about -28.13^{0}C in 2000; then, it increases in 2020 i.e., -24.04^{0}C. D is -31.91^{0}C in 2000 and it's also increases in 2020 i.e., -27.40^{0}C respectively (Figure-7).

Table 4: Minimum and Maximum LST in all buffer distances

Buffer Distance	2000		2008		2013		2020	
	min	max	min	max	min	max	min	max
A (0-5Km)	-4.04	31.65	1.37	28.35	3.95	28.78	-5.87	27.49
B (5-10km)	-18.45	31.65	-11.56	34.46	-8.71	28.89	-16.58	30.88
C (10-15km)	-28.13	30.83	-19.11	33.66	-15.19	29.73	-24.04	30.27
D (15-20km)	-31.91	31.65	-24.54	32.05	-22.59	28.95	-27.4	35.69

Relative change of LST:

It can be observed that the relative change in land surface temperature from 2000 to 2020 indicates that LST decreased about -13.6 % in some areas that is mainly in barren land which is near by glacier area, while the LST is increased by 0-8% in the overall study area (Figure-12). The major increase of 2-8% in LST can be observed mainly in glacier/snow and built-up areas.

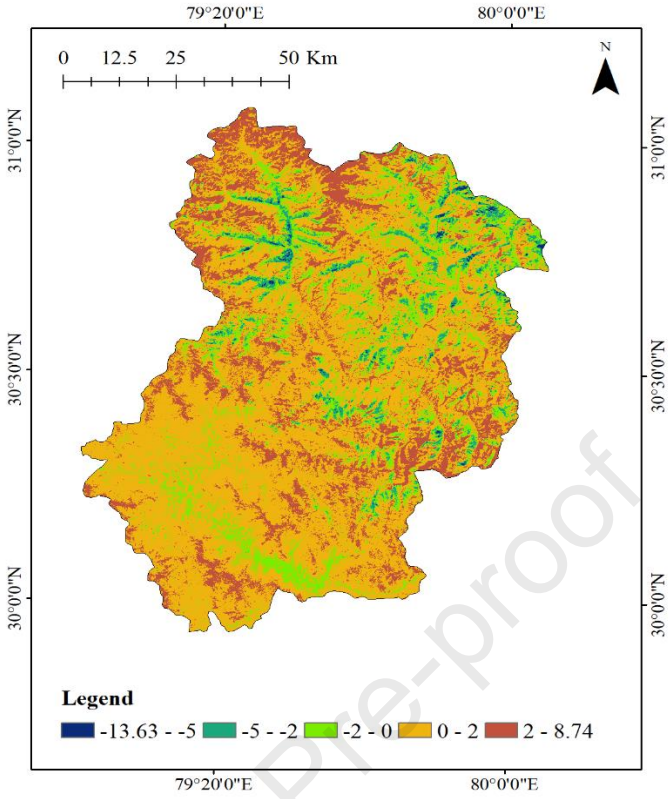

Figure 12: Relative change of Land Surface Temperature

Land use Land cover change

Spatial and temporal evaluation of land use land cover change covering nine classes, viz.- barren land, dense forest, built-up, water bodies, fallow land, vegetation, snow/glacier, other features and shadow of 2000 and 2020 are shown in figures-13 & 14.

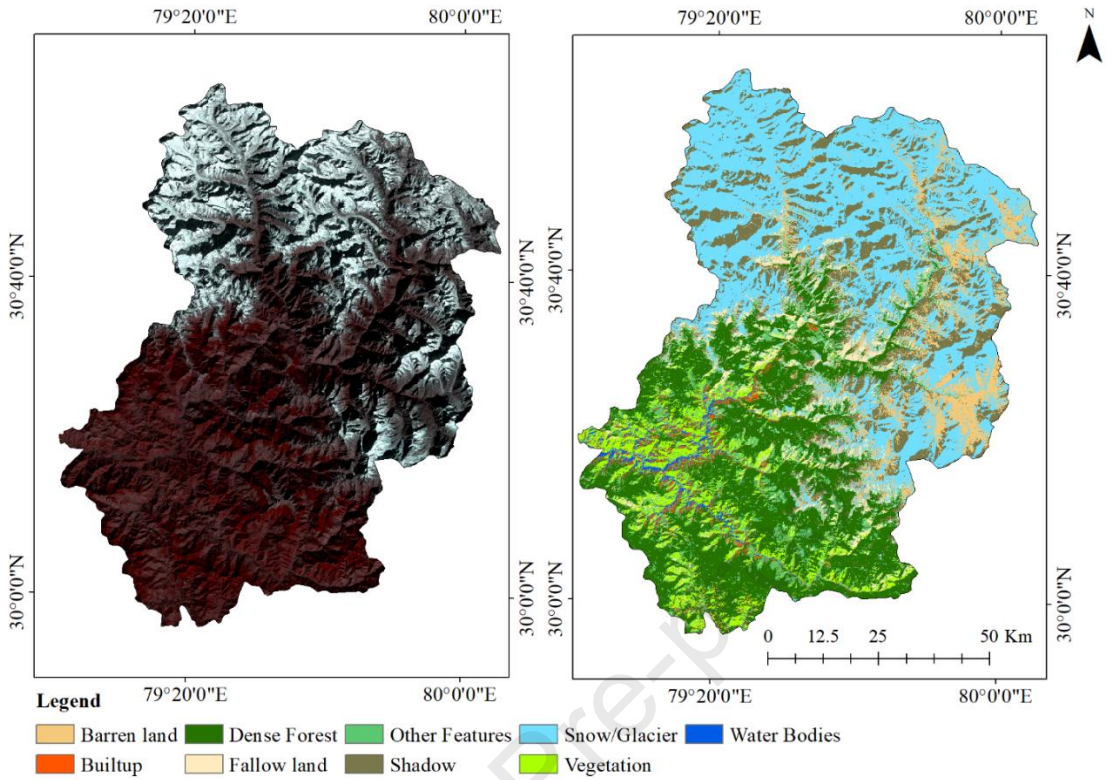

Figure 13: Land use land cover of Chamoli district 2000

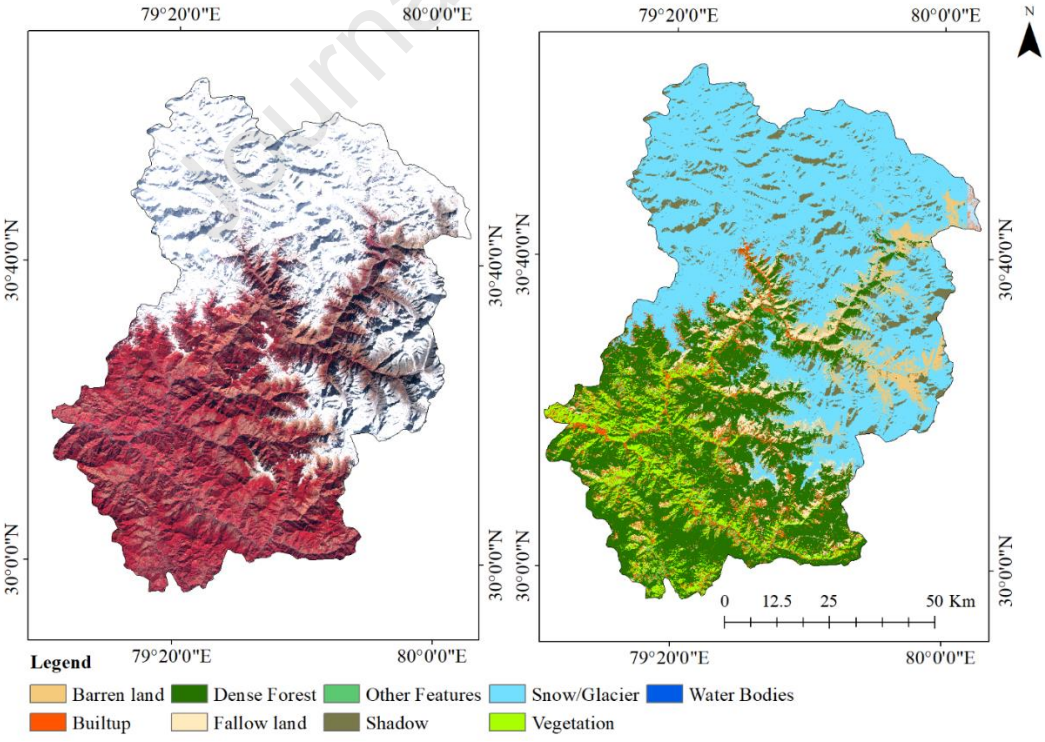

Figure 14: Land use land cover of Chamoli district 2020

Table 5: Statistical analysis of land use land cover change

Class Name	2000 (Km^2)	Area %	2020 (Km^2)	Area %
Built-up	552.58	7.27	1094.15	14.39
Water Bodies	155.41	2.04	103.78	1.36
Dense Forest	1920.51	25.26	1843.55	24.24
Vegetation	290.81	3.82	385.88	5.07
Fallow land	671.33	8.83	307.24	4.04
Other Features	732.09	9.63	138.96	1.83
Snow/Glacier	2610.07	34.32	3039.52	39.97
Shadow	434.00	5.71	446.46	5.87
Barren land	237.19	3.12	244.46	3.21
Total	7604	100	7604	100

Spatial analysis of land use land cover pattern has been extracted using supervised classification. The land use land cover classification results indicated that built-up area occupied 7.27% in 2000 whereas it increased to 14.39% in 2020; dense forest was occupied about 25.26% in 2000 and 24.24% in 2020; water bodies covered 2.04 % in 2000 which has reduced to 1.36 % in 2020; vegetation covered 3.82% in 2000 and 5.07% in 2020; fallow land was about 8.83% in 2000 and 4.04% in 2020; snow/glacier covered 34.32% of the area in 2000 and 39.97% in 2020; whereas barren land was about 3.12 % in 2000 and 3.21% in 2020; other features occupied about 9.63% in 2000 and 1.83% in 2020 (Table-5).

Inventory of Glacial Lakes in Chamoli district:

Glacial lake has been identified using Landsat satellite image and Google Earth image. A total of ~500 glacial lakes has been identified in the district; whereas, some of the studies reveals that there are more than 700 lakes including large, small and very small glacial lakes (Glacial Lakes of Uttarakhand, IIRS, ISRO, 2020). Bhambri et al. (2015) identified 1266 glacial lakes in Uttarakhand state using satellite imageries of the years 2011-2013; among those, 809 glacier lakes are classified as ice-dammed lakes (supra glacial lakes), 329 glacial lakes are identified as moraine -dammed lakes, 125 are identified as glacier erosion lake and rest of the glacial lakes are classified as other glacial lake. Features of lakes and associated glacier have a crucial role in determining GLOF; for instances, lake feeding source, proximity to glacier, glaciers snout, steepness, lake elevation, glacier calving, evolutionary pattern etc. (Shukla et al., 2018; Huggel et al., 2002; ICIMOD 2011). Elevated lakes with a higher force of gravity viz. greater than 3500 m are

susceptible to GLOF (Mohanty and Maiti, 2021; ICIMOD, 2011; Lu et al., 1999). As a consequence of increase in lake discharge, expansion rate of lakes at steep slopes are high as compared to low gradient lakes. The results indicate that 40.92% of the glacial lakes lies in 5000-6000 m elevation, 57.91% of the glacial lakes lies in 4000-5000 m elevation and 1.15% of the glacial lakes lies in 3000-4000 m elevation (Table-6). It was observed that 20.65% of the glacial lakes identified in the study area are fed by the glaciers. They are found to be in contact with the glaciers or in the vicinity of the glaciers (~500 m) also known as pro-glacial lakes while the rest of the lakes are unconnected glacial lakes or supraglacial lakes. These lakes were found to be at an elevation > 4600 m. Thus, making it highly vulnerable.

Table 6: Elevation profiling of Glacial lakes

Sl. No.	Elevation (m)	Percentage of Lakes
1.	3000-4000	1.15 %
2.	4000-5000	57.91 %
3.	5000-6000	40.92 %

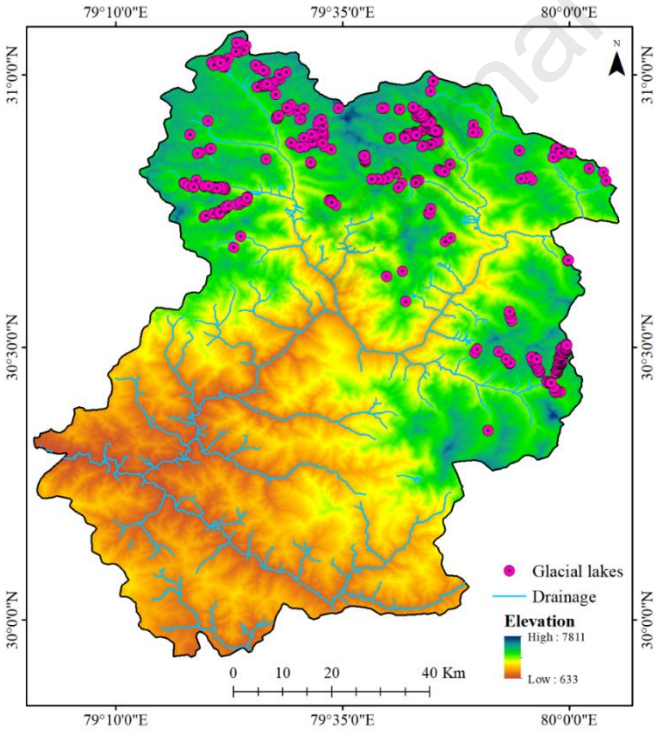

Figure 16: Glacial lakes in Chamoli district

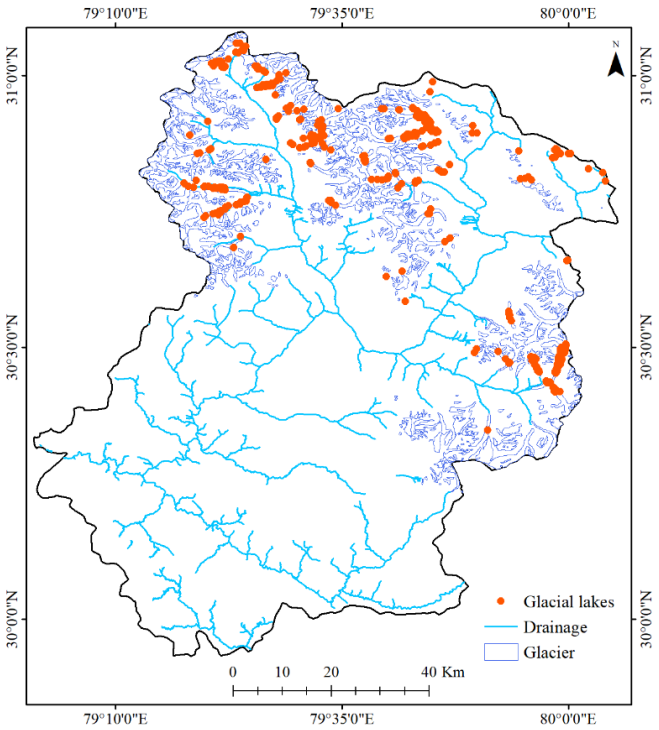

Figure 17: Map showing glacial lakes along with glacier in Chamoli district (Data Source: Randolph Glacier Inventory)

373 ***Implications of Glacial lakes' characteristics***

374 In the study area, three types of lakes have been identified viz., Glacier fed lakes (GFL);
375 supraglacial lakes (SGL) and Unconnected glacial lakes (UGL). The proglacial and Ice marginal
376 lakes have been merged as Glacier fed lakes (GFL). The study reveals that the percentage of SGL
377 are highest in the region (57.14%) followed by unconnected lakes (22.20%) and glacier fed lakes
378 (20.65%) (Table 7). Moreover, most of the SGL are found to be at lower elevation (3880-5710m
379 ASL) as compared to unconnected (4252-5721 m ASL) and Glacier fed lakes (4108-5789m ASL).

380 **Table 7: Different types and numbers of lakes with respect to elevation**

Sl. No.	Types of Lake	No. of Lakes	Elevation (m)	Percentage of lakes
1.	Glacier fed Lakes (Pro-Glacial lakes (PGL) or Ice Marginal Lakes (IML))	107	4108-5789	20.65
2.	Supraglacial Lakes (SGL)	296	3880-5710	57.14
3.	Unconnected Glacial lakes (UGL)	115	4252-5721	22.20

381 It is also seen with the help of google earth images that most of the SGL are in the lower ablation
382 zones of the glaciers (tongue of the glacier) as well as in debris covered glaciers; similar
383 observations were made by other researchers too (Benn et al., 2001, 2012; Westoby et al., 2014;
384 Shukla et al., 2018). This will act as a hotspot for ablation and can locally enhance melting rates
385 by a factor of three to 13 compared to the surrounding debris-covered ice (Buri and others, 2016a;
386 Brun and others, 2018). Therefore, the increasing number of SGL can be an alarm to the valley as
387 these SGL are a hotspot of high risk melting which can lead to sudden outburst after several years
388 or with any onset of extreme weather event, for instance., Chorabari glacial lake outburst (Sakai
389 et al., 2000; Benn et al., 2012; Das et al., 2015; Thompson et al., 2016; Miles et al., 2017). The
390 water from SGL can seep through the glacier ice, lubricating the glacier-bed and sometimes
391 resulting in glacier surges (sudden advances of glacier ice). It could also lead to collapse of roof
392 of englacial conduit which would accelerate the ablation process thus can trigger GLOFs (Shukla
393 et al., 2018). Moreover, merging of SGL could result in the formation of much larger lakes and
394 proglacial lakes behind the loose moraine which increases the potential for outburst (Field et al.,

2012; Worni et al., 2014; Gurung et al., 2017) (For instance, figure 18). Furthermore, the proglacial lakes also have severe implications related to the glacier health and human well-being which may instigate the calving process leading to an increased terminus disintegration and higher retreat (Warren and Kirkbride, 1998; Benn et al., 2001, 2012; Sakai, 2012). Moreover, the lakes which have stable surface drainage are less vulnerable to outburst floods than glacial lakes with an underground drainage system. The reasons behind this vulnerability are erosion, breach formation and blocking of intra-moraine channels by thermokarst process, which lead to lake overflow (Erokhin et al., 2018; Narama et al., 2018; Petrakov et al., 2012, 2020; Schmidt et al., 2020).

Change in Characteristics of Glacial lakes:

The glacial lakes are changing continuously for the past 4 decades (2000-2020) (Figure 18). The growth of glacial lakes and the melting of subaqueous ice or ice cliffs are both influenced by lake and its surrounding temperature (Sakai et al., 2009; Benn et al., 2012). Higher insolation causes increased melting of snow/ice, which might get trapped behind the natural barriers or collect in pre-existing topographic depressions, resulting in the formation of different types of lakes (Shukla et al., 2018).

Table 8: Volume (in m^3 x 10^6) of the Glacial Lake from 2000 to 2020

Glacial Lake	2000	2008	2013	2020
GL 1	1.59	2.79	2.99	4.03
GL 2	5.77	8.11	8.14	19.68
GL 3	0.97	1.14	1.05	1.78

Figure-18 shows three major lakes undergoing changes over past few decades. GL1 shows that the SGL is expanding over the time period hence the volume has been increased by 2.44 m^3 x 10^6 volume from 2000 to 2020 (Table 8). GL2 is another SGL which volume is continuously increasing which resulted in increase in volume by 13.91 m^3 x 10^6 from 2000 to 2022; whereas, the findings indicates that if glaciers are melting continuously then it's possible that GL2 can be transformed into a Proglacial lake due to the merging of small glaciers. GL3 is Proglacial lakes which has also experienced increase in its volume by 0.80 m^3 x 10^6 during the studied period.

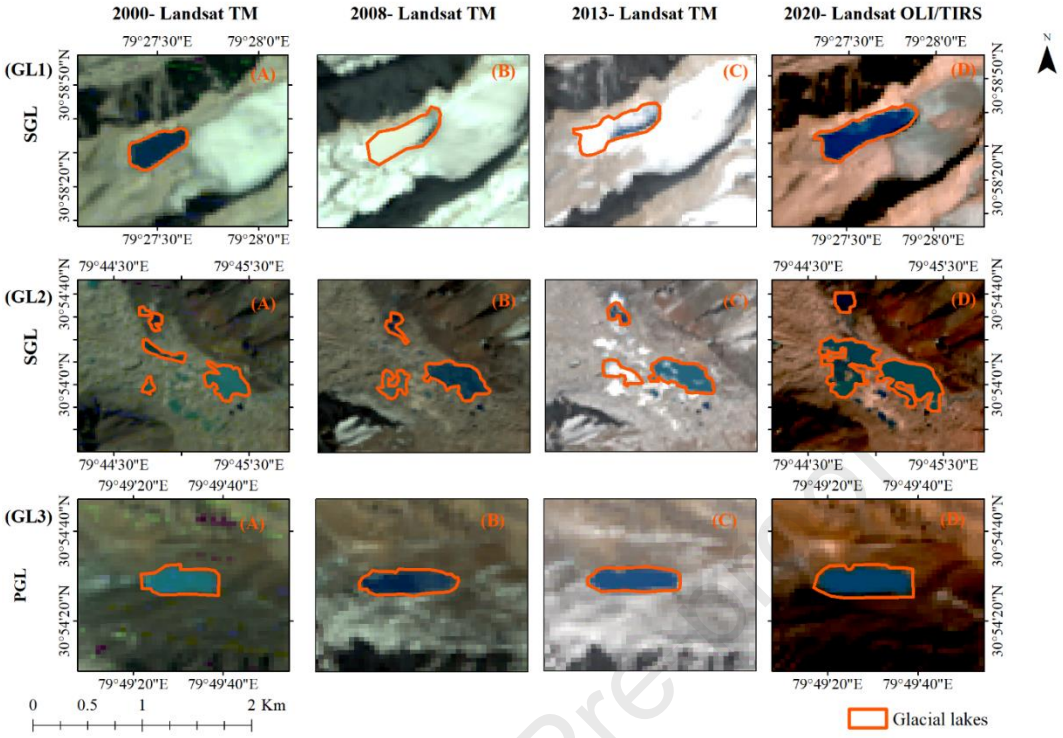

419 **Figure 18: Map showing change in Supraglacial Lakes (SGL) and Proglacial Lakes (PGL),**
420 **from 2000 to 2020 in Chamoli district**

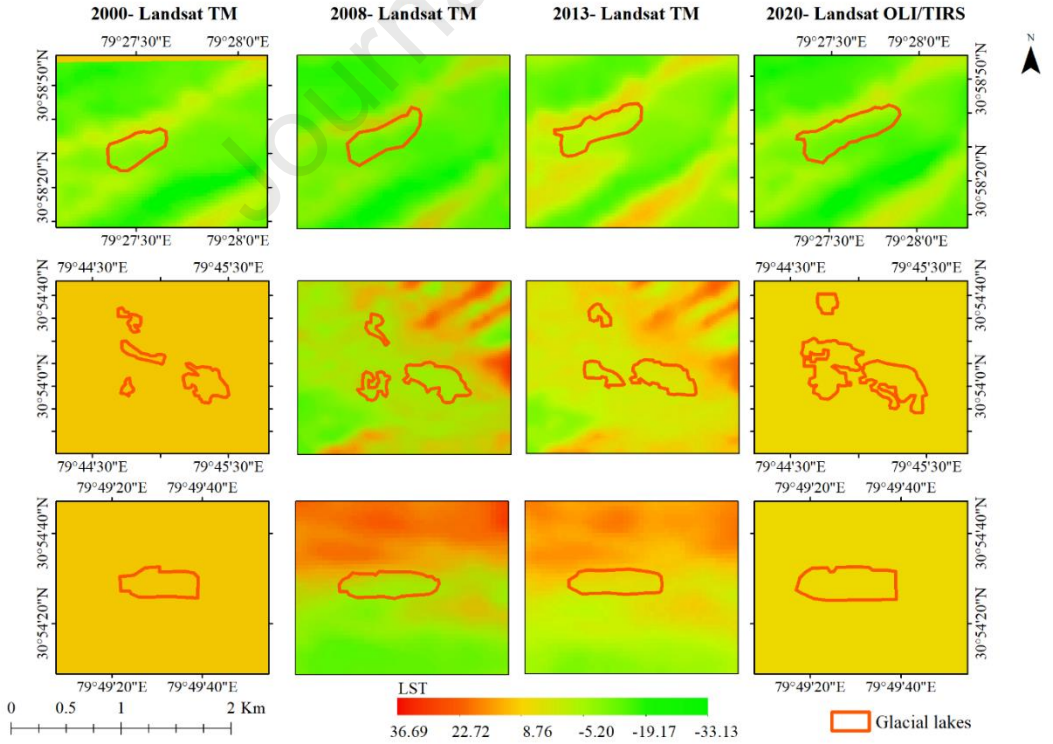

Figure 19: Map showing change in LST in Glacial lakes from 2000 to 2020 in Chamoli district

Previous studies imply that with the increase in temperature in the glaciated regions, the heated water in the lakes expands the englacial conduit, which drains water from the lakes and causes internal ablation (Sakai et al., 2000). It has been observed in this study that with the increase in temperature over the years, the glacial lakes are increasing in terms of area. For instance, figure 19 illustrates the lakes and their surrounding land surface temperature. It is clearly seen that the temperature of the lake and nearby areas has increased over the years and so is the area of the lakes with the passage of year from 2000 to 2020. The change in glacial lakes mainly due to the increase in heat intensity and environmental degradation. Since the observation of LST in the surrounding region of Glacial lakes (Figure 19) indicates that LST may one of the reasons to increase the volume of lake over the time period. GL 1 indicates that the LST has been increased in 2013 from 2000, similarly in GL2 and GL3, the LST reaches the high value in 2008 and 2013 i.e., ~36.69 ^{o}C.

Seismicity in study area

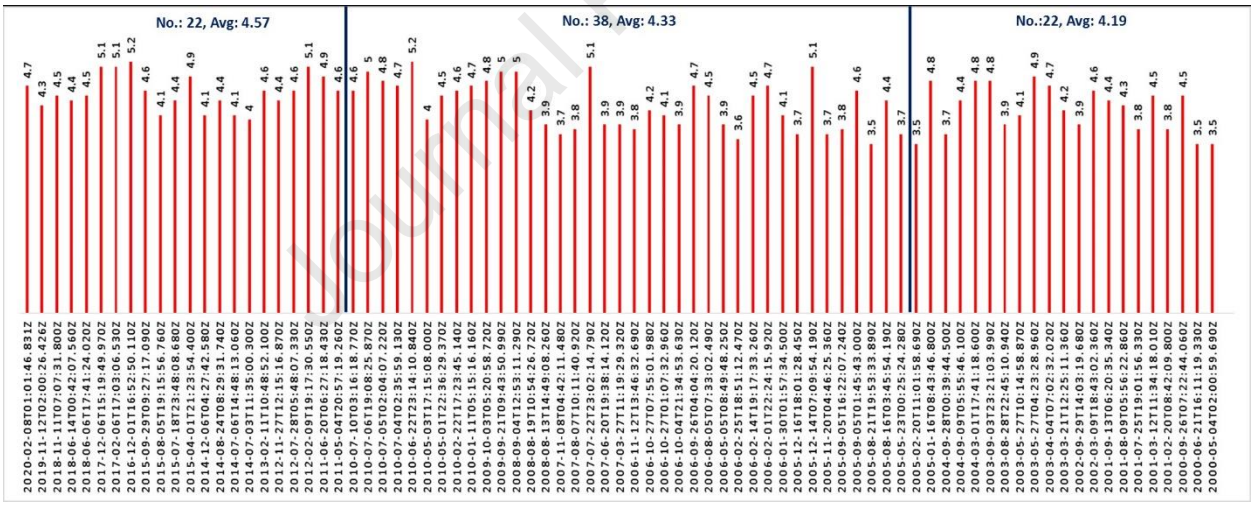

Figure 20: Occurrence of seismic events in and around study region (2000-2020)

Uttarakhand being located in high seismicity zone, the state has experienced two high magnitude earthquakes (Uttarkashi and Chamoli) and many minor and medium shakes, which is due to the presence of several tectonic discontinuities in the region, viz.- Himalayan Frontal Fault; HFF, Main Boundary Thrust; MBT and Main Central Thrust; MCT. Figure-20 shows the seismic activities in the region since 2000. The magnitude of seismic events is increased after 2008; whereas in year 2000 to 2005 the average magnitude of seismic events is 4.19 further from 2005

to 2010 is 4.33 and 2011 to 2020 is 4.57. From 2000 to 2005; the magnitude of seismic events is ranging from 3.5 to 4.8 whereas from 2005 to 2008; it ranges from 3.5 to 5.1 and from 2008 to 2020 the magnitude is ranging from 3.7 to 5.2. The results also indicates that during the recent years, from 2016 to 2020, the occurrence of higher magnitude earthquakes was increasing as compared to previous years.

There are evidences where glacier bursts are prompted by seismic activities of the region. Association of seismic activities with GLOF induced hazards are reported in Himalayan region (Maurer et al. 2020; Dugar and Dahal, 2014). Increase in seismic activity and a build-up of hydrological pressure also leads to glacier burst. Hence the monitoring of seismic events in glacier region demonstrates various surface activities such as river bedload transport and debris flow further indicates the seismic results ability to provides a specific insight on flood mechanism from seismic records. (Badoux et al., 2009; Burtin et al., 2008; Burtin et al., 2016; Cook et al., 2018; Schmandt et al., 2013). A scenario of Tsho Rolpa, which is highly affected with GLOFs and one of the most highly vulnerable risk zones in Nepal where GLOFs are damned by moraine banks and these moraines are inherently unstable structures that are easily exacerbated by earthquakes or landslides. Since the monitoring of seismic activities is needed to control the damage due to GLOFs.

Discussions

Chamoli district is one of the major eco-sensitive zones of Himalayan region (Kumar et al., 2018). The present analysis shows the change in environmental parameters and their impacts in eco-sensitive zone. Since, the various geoclimatic parameters have been analysed for Chamoli district including Maximum and Minimum Temperature, Relative Humidity, Land use Land Cover change, Land Surface Temperature and Seismicity. The results indicate that built-up area has increased from the year 2000 to 2020 by 541.57 Km^2 which leads to a range of disturbances in the eco-sensitive zone. Anthropogenic pressure in the form of urbanization and consequent decrease in forest cover are major threats for the pristine ecosystems of the district, making it vulnerable to occurrence of natural hazards as well as human induced intensity of damage. Study findings show that forest cover has been decreased by 1.02% from 2000 to 2020. Other research reveals that the annual rate of change in forest cover was 0.22% from 1976-1998 and 0.27% from 1998-2014 in the region (Batar et al., 2017). The loss of forest and fallow land is one of the major indicators

474 which show transition to built-up area. As per the results, major changes occurred in fallow
475 land, other features, dense forest and also in barren land. The forest cover has been degraded due
476 to anthropogenic activities and natural climatic factors, which impacts are also visible in form of
477 increasing LST. Increase in LST mainly due to the increase in built-up area for human settlement
478 and construction of hydroelectric power plants. Maximum and Minimum temperature results
479 reveal that the minimum temperature is gradually increasing while maximum temperature is
480 decreasing. Increase in temperature and incessant rainfall events facilitates further melting and
481 increase in number and volume of the lakes (Reynolds, 2000; Benn et al., 2012; Field et al., 2012;
482 Field 2014; Riaz et al. 2014; Crammer 2014; Thompson et al., 2016; Pandey et al., 2021; Ahmed
483 et al, 2021). The findings are suggestive of probable threats from changing ambient as well and
484 land surface temperature which may lead to frequent and intensified glacial lake related hazards.

485 According to GSI from 2014-16, 486 glacial lakes of Uttarakhand were identified and 13 lakes
486 were reported for highly vulnerable to GLOF and close to Rishiganga and Dhauliganga valley.
487 As per the ICIMOD, there are 1439 glaciers and 127 glacial lakes in Uttarakhand (Table-9). In
488 Himachal Pradesh, there are 2554 glaciers and 156 glacial lakes- according to ICIMOD 16 lakes
489 are considered as highly vulnerable risk zone (Bhagat et al., 2004). In a study of Sah et al., 2005
490 demonstrated that none of the lakes are potentially vulnerable or dangerous. Recent incidents on
491 17th June 2013, Kedarnath GLOF and also on 7th Feb 2021 massive GLOF disaster have many
492 consequential damages. The average surface temperature is increasing from Little Ice Age which
493 is ranges in between 0.3 ^{O} C to 0.6^{O}C (ICIMOD 2007). As per the IPCC report 2007, temperature
494 will be increased in Himalayan region from 1^{O} to 6^{O}C by 2100 (Banerjee et al., 2013). Whereas
495 the recent IPCC report (IPCC-AR-6, 2021) has reported with high confidence that warming has
496 occurred in the Himalayas and has increased with altitude. Such elevation-dependent warming has
497 the potential to change glacier equilibrium and snow line at a faster rate, which indicates alarming
498 consequences in the future.

499 **Table 9: Glaciers, glacial lakes and potentially dangerous lakes in IHR covered by**
500 **Uttarakhand state (Source: ICIMOD)**

River Basin	Glaciers			Glacial Lakes		
	Number	Area (sq.km)	Ice reserves (cu.km)	Number	Area (sq.km)	Potentially dangerous
Uttaranchal (Uttarakhand)						

Yamuna	124	173	17.88	20	0.17	0
Bhagirathi	393	1034	143.41	32	0.44	0
Alaknanda	540	1675	191.36	54	1.37	0
Kali	382	1178	122.78	21	0.51	0
Total	1439	4060	475.43	127	2.49	0
Tista river basin (Total)	285	577	64.78	266	20.2	14

Various scientific studies in Himalayan region revealed that a large number of lakes are capable to produce GLOFs which can cause downstream damage (Dubey and Goyal 2020; Worni et al., 2013). In the Trans-Himalayan of Ladakh region, it has been observed that a proglacial lake extended from 3.06 ha in 1969 to 11 ha in 2019 and 25% of the lake drained with a peak discharge of $470m^3S^{-1}$ which inundating an area of ~$4Km^2$ in Gya Village. It was mentioned that breaching of terminal moraine might be 5.5 times greater than the 2014 GLOF event in Gya, Ladakh (Majeed et al., 2020). In a recent study, Dubey and Goyal (2020) analysed the potential downstream impact of 329 lake in Indian Himalayan region where they indicated that 36 lakes are susceptible to avalanche impact zones. Moreover, Worni et al. (2013) mapped 251 glacial lakes where 12 lakes are critical and 93 are susceptible for lake outburst and potential downstream exposure. A study in Uttarakhand reveals that 16 out of 78 tehsils are vulnerable to GLOFs. Scientific evaluation by Wadia Institute of Himalayan Geology stated that Dehradun has 1266 glacial lakes; where 10-11 Moraine Dam glacial lakes are highly vulnerable to lake outburst. Recent studies in climate change reveal that Indian Himalayan Glaciers are retreating (Taloor et al., 2021). It was mentioned that 1/3rd of Uttarakhand is at high risk of glacier floods. 5000 glacial lakes were reported and identified in Indian Himalayan region where the analysis reported that 500 glacier lakes in Uttarakhand at risk of a glacial outburst.

A new Intergovernmental Panel on Climate Change (IPCC) report 6 warns that unless there are immediate rapid and large-scale reductions in greenhouse gas emissions, limiting warming to close to 1.5^o C or even 2^o C will be beyond reach. The reports also envisaged that there will be an increase in frequency of heat waves in the coming decade with the rise in global warming. However, the increase in Snow/Glacier cover by 5.65% has made a positiveness in this eco-sensitive zone. Snow/Glacier cover maintains the pattern of cooling and heating of the earth's surface. Nepal et al., 2021 projected that snow cover area is reduced by 25% by end of century

in Western Himalayan region. Hence the increase in snow cover in Chamoli districts provides a encouraging indication in maintaining the balanced earth's temperature.

Increase in built-up as well as increase in construction activities of Tapovan-Vishnugad Hydroelectric power plant might have generated several disturbances in the natural landscape of Chamoli district. The results of LST suggested that the minimum and maximum land surface temperature increased from 2000 to 2020. However, the construction of Tapovan-Vishnugad Hydroelectric power plant was started in November 2006. For the analysis, we have taken the data after 2 years from the beginning of construction of the power plant. The results of LST shows that LST has increased near the buffer zone in 2008 as compared to 2000. Power production of the hydroelectric powerplant was expected to begin in 2012 but due to flash flood in 2013 delayed its production. The diversion tunnel was completely destroyed along with the under-construction cofferdam. Further, the LST was also analysed for the year 2013 that represents the LST has decreased in buffer zone BCD. Further the LST was significantly increasing in Buffer Zone BCD. The relative change of LST exhibits the major changes in glacier and built-up region. These anthropogenic activities and global climate change can be associated as major reasons for creating disturbances in the eco-sensitive zone.

The results of the present studies on changing physical landscape, anthropogenic interventions in sensitive zones, high seismicity in the region, change in climatic parameters as well as land surface temperature are critical aspects with regard to increasing vulnerability to glacial lake related hazards. Recent event of glacial lake outburst flood in Chamoli district on 7th Feb 2021due to avalanche or landslip or cloudburst in the catchment, reveals that glacial lake can cause massive flood with tremendous damage in the downstream. This glacial burst damaged the Hydroelectric power plant in Tapovan and hundreds of people were dead. Hence, continuous and real time monitoring and assessment of glacial lakes is required to analyse the vulnerable zones or threat factors.

Conclusion

The results of the study show that increasing trend of minimum ambient temperature, high seismicity, changing physical landscape and land surface temperature in Chamoli district tend to position the glacial lakes in a more vulnerable status. The changes in the lakes assessed for area and volume provide evidence for the dynamic nature of glacial lakes in the study area, making

556 them prone to outbursts. GLOFs can be discussed in two ways; primarily when moraine banks,
557 deposited rock burst due to earthquake that results in a GLOF and secondly, increase in glacial
558 lake due to glacier retreat or high precipitation. The direct control over these factors cannot be
559 achieved by human action. Nevertheless, damage intensity can be minimized through proper
560 monitoring and development of alarm system. Detailed hydrological mass balance studies can
561 support to identify potential hazard zones. On the other hand, real time monitoring and decision
562 making for developing alarm system can reduce devastation on human population. Rational
563 decision on further anthropogenic landscape change in the region as well curtail future human
564 intervention in the landscape can help in abatement of disaster impacts.

565 **Annexures:**

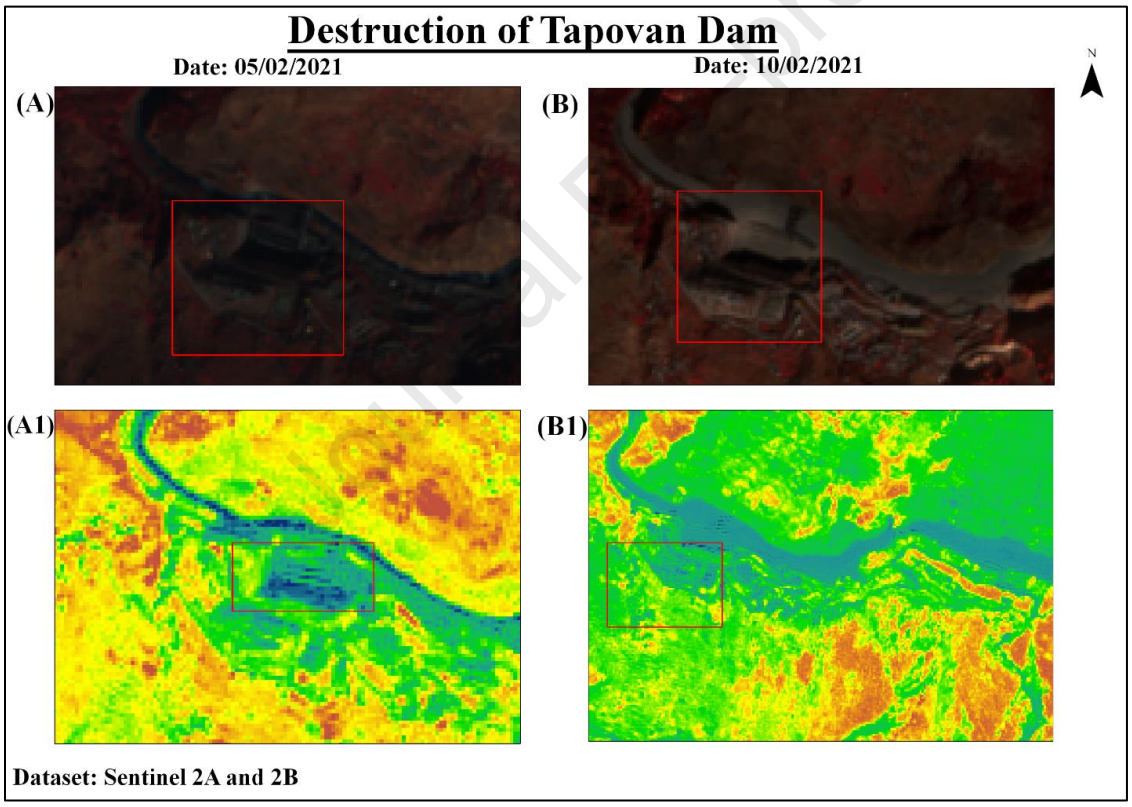

566

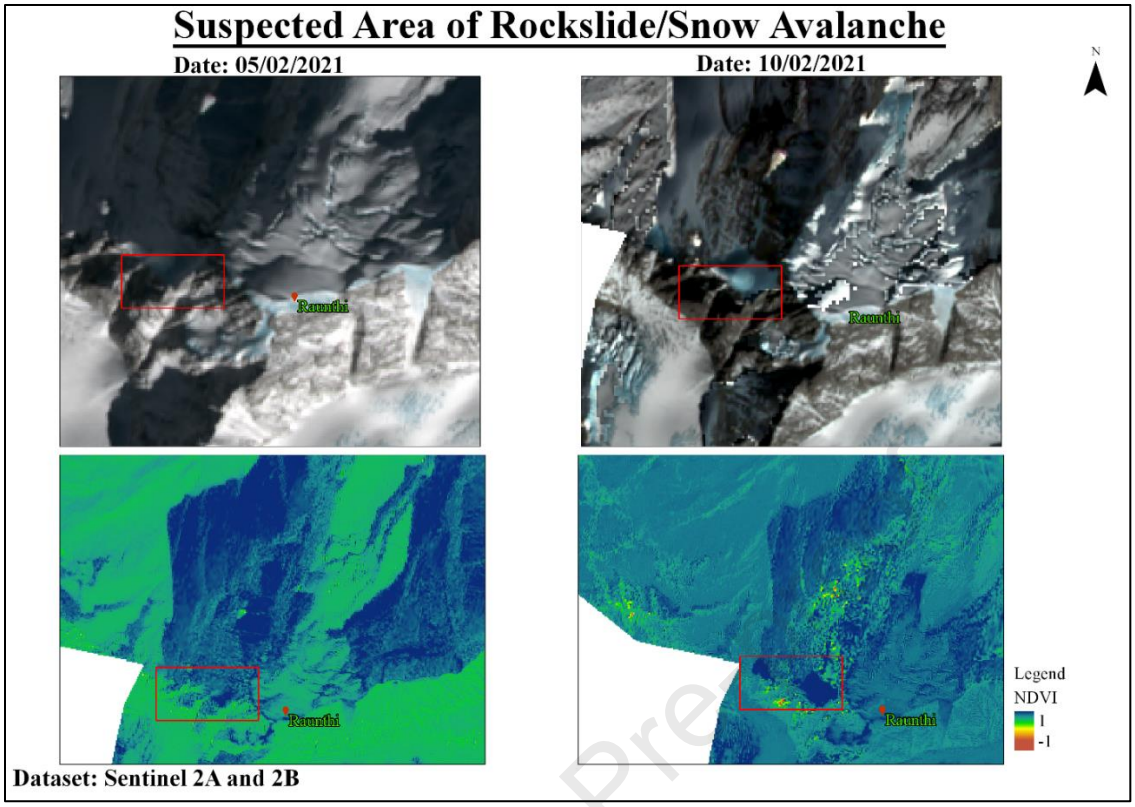

583 **References**

584 Arulbalaji, P., Padmalal, D. and Maya, K., 2020. Impact of urbanization and land surface
585 temperature changes in a coastal town in Kerala, India. *Environmental Earth Sciences*, *79*(17),
586 pp.1-18. https://doi.org/10.1007/s12665-020-09120-1.

587 Badoux, A., Graf, C., Rhyner, J., Kuntner, R. and McArdell, B.W., 2009. A debris-flow alarm
588 system for the Alpine Illgraben catchment: design and performance. *Natural hazards*, *49*(3),
589 pp.517-539. https://doi.org/10.1007/s11069-008-9303-x.

590 Banerjee, A. and Shankar, R., 2013. On the response of Himalayan glaciers to climate change.
591 Journal of Glaciology, 59(215), pp.480-490. doi:10.3189/2013JoG12J130.

592 Benn, D. I., Bolch, T., Hands, K., Gulley, J., Luckman, A., Nicholson, L. I., et al. (2012). Response
593 of debris-covered glaciers in the Mount Everest region to recent warming, and implications for
594 outburst flood hazards. Earth Sci. Rev. 114, 156–174. doi: 10.1016/j.earscirev.2012.03.008.

595 Benn, D. I., Wiseman, S., and Hands, K. A. (2001). Growth and drainage of supraglacial lakes on
596 debris-mantled Ngozumpa Glacier, Khumbu Himal, Nepal. J. Glaciol. 47, 626–638. doi:
597 10.3189/172756501781831729.

598 Bhagat, R.M., Kalia, V., Sood, C., Mool, P.K., Bajracharya, S., 2004. Inventory of glaciers and
599 glacial lakes and the identification of potential glacial lake outburst floods (GLOFs) affected by
600 global warming in the mountains of the Himalayan region: Himachal Pradesh Himalaya, India.
601 Unpublished project report, ICIMOD, Kathmandu, Nepal.

602 Bhambri, R., Mehta, M., Dobhal, D.P. and Gupta, A.K., 2015. *Glacier lake inventory of*
603 *Uttarakhand*. Wadia Institute of Himalayan Geology.

604 Bhutiyani, M.R., Kale, V.S. and Pawar, N.J., 2007. Long-term trends in maximum, minimum and
605 mean annual air temperatures across the Northwestern Himalaya during the twentieth
606 century. *Climatic Change*, *85*(1), pp.159-177. https://doi.org/10.1007/s10584-006-9196-1.

607 Borgaonkar, H.P., Ram, S. and Sikder, A.B., 2009. Assessment of tree-ring analysis of high-
608 elevation Cedrus deodara D. Don from Western Himalaya (India) in relation to climate and glacier
609 fluctuations. *Dendrochronologia*, *27*(1), pp.59-69. https://doi.org/10.1016/j.dendro.2008.09.002.

610 Brun, F., Wagnon, P., Berthier, E., Shea, J. M., Immerzeel, W. W., Kraaijenbrink, P. D., ... &
611 Arnaud, Y. (2018). Ice cliff contribution to the tongue-wide ablation of Changri Nup Glacier,
612 Nepal, central Himalaya. The Cryosphere, 12(11), 3439-3457. https://doi.org/10.5194/tc-12-3439-
613 2018.

614 Buri, P., Miles, E. S., Steiner, J. F., Immerzeel, W. W., Wagnon, P., & Pellicciotti, F. (2016). A
615 physically based 3-D model of ice cliff evolution over debris-covered glaciers. Journal of
616 Geophysical Research: Earth Surface, 121(12), 2471-2493.
617 https://doi.org/10.1002/2016JF004039.

618 Burtin, A., Bollinger, L., Vergne, J., Cattin, R. and Nábělek, J.L., 2008. Spectral analysis of
619 seismic noise induced by rivers: A new tool to monitor spatiotemporal changes in stream

hydrodynamics. *Journal of Geophysical Research: Solid Earth*, *113*(B5). https://doi.org/10.1029/2007JB005034.

Burtin, A., Hovius, N. and Turowski, J.M., 2016. Seismic monitoring of torrential and fluvial processes. *Earth Surface Dynamics*, *4*(2), pp.285-307. https://doi.org/10.5194/esurf-4-285-2016.

Census of India, 2011. Census of India, Ministry of Home Affairs, office of the Registrar

Chen, X. L., Zhao, H. M., Li, P. X., & Yin, Z. Y. (2006). Remote sensing image-based analysis of the relationship between urban heat island and land use/cover changes. *Remote sensing of environment*, *104*(2), 133-146. https://doi.org/10.1016/j.rse.2005.11.016.

Chen, Y., Xu, C., Chen, Y., Li, W., Liu, J., 2010. Response of glacial-lake outburst floods to climate change in the Yarkant River basin on northern slope of Karakoram Mountains, China. Quaternary International 226 (1), 75e81. https://doi.org/10.1016/j.quaint.2010.01.003.

Chen, Y.H., Wang, J. and Li, X.B., 2002. A study on urban thermal field in summer based on satellite remote sensing. *Remote Sensing for Land and Resources*, *4*(1), pp.55-59. DOI: 10.6046/gtzyyg.2002.04.12.

Cheval, S. and Dumitrescu, A., 2009. The July urban heat island of Bucharest as derived from MODIS images. Theoretical and applied climatology, 96(1), pp.145-153. https://doi.org/10.1007/s00704-008-0019-3.

Chevallier, P., Pouyaud, B., Suarez, W. and Condom, T., 2011. Climate change threats to environment in the tropical Andes: glaciers and water resources. *Regional Environmental Change*, *11*(1), pp.179-187. https://doi.org/10.1007/s10113-010-0177-6.

Clague, J.J., Evans, S.G., 1993. Historic catastrophic retreat of Grand Pacific and Melbern Glaciers, St. Elias mountains: an analogue for late Pleistocene decay of the Cordilleran Ice Sheet? Journal of Glaciology 39, 619e624.

Cook, K.L., Andermann, C., Gimbert, F., Adhikari, B.R. and Hovius, N., 2018. Glacial lake outburst floods as drivers of fluvial erosion in the Himalaya. *Science*, *362*(6410), pp.53-57. https://doi.org/10.1126/science.aat4981.

Cook, S.J. and Quincey, D.J., 2015. Estimating the volume of Alpine glacial lakes. Earth Surface Dynamics, 3(4), pp.559-575. https://doi.org/10.5194/esurf-3-559-2015.

Crago, R., Sugita, M. and Brutsaert, W., 1995. Satellite-derived surface temperatures with boundary layer temperatures and geostrophic winds to estimate surface energy fluxes. *Journal of Geophysical Research: Atmospheres*, *100*(D12), pp.25447-25451. https://doi.org/10.1029/95JD00724.

Cramer, W., Yohe, G.W., Auffhammer, M., Huggel, C., Molau, U., da Silva Dias, M.A.F., Solow, A., Stone, D.A., and Tibig, L. 2014. Detection and attribution of observed impacts. In: Climate change 2014: Impacts, adaptation, and vulnerability. Part a: Global and Sectoral aspects. Contribution of Working group II to the fifth assessment report of the Intergovernmental Panel on climate change [Field, C.B., V.R. Barros, D.J. Dokken, K.J. Mach, M.D. Mastrandrea, T.E. Bilir,

M. Chatterjee, K.L. Ebi, Y.O. Estrada, R.C. Genova, B. Girma, E.S. Kissel, A.N. Levy, S. MacCracken, P.R. Mastrandrea, and L.L. White (eds.)]. Cambridge University Press, Cambridge, United Kingdom and New York, NY, USA, pp. 979-1037.

Dadras, M., Shafri, H.Z., Ahmad, N., Pradhan, B. and Safarpour, S., 2015. Spatio-temporal analysis of urban growth from remote sensing data in Bandar Abbas city, Iran. The Egyptian Journal of Remote Sensing and Space Science, 18(1), pp.35-52. https://doi.org/10.1016/j.ejrs.2015.03.005.

Das, D.N., Chakraborti, S., Saha, G., Banerjee, A. and Singh, D., 2020. Analysing the dynamic relationship of land surface temperature and landuse pattern: A city level analysis of two climatic regions in India. *City and Environment Interactions*, *8*, p.100046. https://doi.org/10.1016/j.cacint.2020.100046.

Das, S., Kar, N. S., & Bandyopadhyay, S. (2015). Glacial lake outburst flood at Kedarnath, Indian Himalaya: a study using digital elevation models and satellite images. Natural Hazards, 77(2), 769-786. https://doi.org/10.1007/s11069-015-1629-6.

Degefu, M.A. and Bewket, W., 2014. Variability and trends in rainfall amount and extreme event indices in the Omo-Ghibe River Basin, Ethiopia. *Regional environmental change*, *14*(2), pp.799-810. https://doi.org/10.1007/s10113-013-0538-z.

Deng, C. and Wu, C., 2013. Examining the impacts of urban biophysical compositions on surface urban heat island: A spectral unmixing and thermal mixing approach. *Remote Sensing of Environment*, *131*, pp.262-274. https://doi.org/10.1016/j.rse.2012.12.020.

Dimri, A.P. and Dash, S.K., 2012. Wintertime climatic trends in the western Himalayas. *Climatic Change*, *111*(3), pp.775-800. https://doi.org/10.1007/s10584-011-0201-y.

Dubey, S. and Goyal, M.K., 2020. Glacial lake outburst flood hazard, downstream impact, and risk over the Indian Himalayas. *Water Resources Research*, *56*(4), p.e2019WR026533. https://doi.org/10.1029/2019WR026533.

Dugar, S. and Dahal, V., 2015. Analysis of Spatial and Temporal Trends of Climate Induced Hazards in Eastern Nepal. Participatory Community Assessment for Priority Problem Diagnosis in Bajura District, Nepal: What Matters Most–Poverty or Climate Change? p.339.

Erokhin, S.A., Zaginaev, V.V., Meleshko, A.A., Ruiz-Villanueva, V., Petrakov, D.A., Chernomorets, S.S., Viskhadzhieva, K.S., Tutubalina, O.V. and Stoffel, M., 2018. Debris flows triggered from non-stationary glacier lake outbursts: the case of the Teztor Lake complex (Northern Tian Shan, Kyrgyzstan). *Landslides*, *15*(1), pp.83-98. https://doi.org/10.1007/s10346-017-0862-3.

Field, C.B., V. Barros, T.F. Stocker, D. Qin, D.J. Dokken, K.L. Ebi, M.D. Mastrandrea, K.J. Mach, G.K. Plattner, S.K. Allen, M. Tignor, and P.M. Midgley. 2012. Managing the risks of extreme events and disasters to advance climate change adaptation. A Special Report of Working Groups I and II of the Intergovernmental Panel on Climate Change. Cambridge, UK, and New York, NY: Cambridge University Press.

Field, C.B., V.R. Barros, D.J. Dokken, K.J. Mach, M.D. Mastrandrea, T.E. Bilir, M. Chatterjee, K.L. Ebi, Y.O. Estrada, R.C. Genova, B. Girma, E.S. Kissel, A.N. Levy, S. MacCracken, P.R. Mastrandrea, L.L. White, and editors. 2014. Climate change 2014: Impacts, adaptation, and vulnerability. Part a: Global and Sectoral aspects. Contribution of Working group II to the fifth assessment report of the Intergovernmental Panel on climate change. Cambridge, UK, and New York, NY: Cambridge University Press.

Fonseka, H.P.U., Zhang, H., Sun, Y., Su, H., Lin, H. and Lin, Y., 2019. Urbanization and its impacts on land surface temperature in Colombo metropolitan area, Sri Lanka, from 1988 to 2016. *Remote Sensing*, *11*(8), p.957. https://doi.org/10.3390/rs11080957.

Good, E.J., 2016. An in situ-based analysis of the relationship between land surface "skin" and screen-level air temperatures. *Journal of Geophysical Research: Atmospheres*, *121*(15), pp.8801-8819. https://doi.org/10.1002/2016JD025318.

Good, E.J., Ghent, D.J., Bulgin, C.E. and Remedios, J.J., 2017. A spatiotemporal analysis of the relationship between near-surface air temperature and satellite land surface temperatures using 17 years of data from the ATSR series. *Journal of Geophysical Research: Atmospheres*, *122*(17), pp.9185-9210. https://doi.org/10.1002/2017JD026880.

Gurung, D.R., Khanal, N.R., Bajracharya, S.R. et al. Lemthang Tsho glacial lake outburst flood (GLOF) in Bhutan: cause and impact. Geoenviron Disasters 4, 17 (2017). https://doi.org/10.1186/s40677-017-0080-2.

Hachem, S., Duguay, C.R. and Allard, M., 2012. Comparison of MODIS-derived land surface temperatures with ground surface and air temperature measurements in continuous permafrost terrain. *The Cryosphere*, *6*(1), pp.51-69. https://doi.org/10.5194/tc-6-51-2012.

Haeberli, W., Huggel, C., Paul, F., Zemp, M., Shroder, J.F., James, L.A., Harden, C.P. and Clague, J.J., 2013. Glacial responses to climate change. https://doi.org/10.1016/B978-0-12-374739-6.00350-X.

Hu, L. and Brunsell, N.A., 2013. The impact of temporal aggregation of land surface temperature data for surface urban heat island (SUHI) monitoring. *Remote Sensing of Environment*, *134*, pp.162-174. https://doi.org/10.1016/j.rse.2013.02.022.

Hu, Y., Jia, G., 2010. Influence of land use change on urban heat island derived from multi-sensor data. Int. J. Climatol. 30, 1382–1395. https://doi.org/10.1002/joc.1984.

Huggel, C., Kääb, A., Haeberli, W., Teysseire, P. and Paul, F., 2002. Remote sensing based assessment of hazards from glacier lake outbursts: a case study in the Swiss Alps. Canadian Geotechnical Journal, 39(2), pp.316-330. https://doi.org/10.1139/t01-099.

ICIMOD., 2007. The melting Himalayas: regional challenges and local impacts of climates change on mountain ecosystems and livelihoods. Technical paper X. International Centre for Integrated Mountain Development, Kathmandu.

ICIMOD., 2011. Glacial lakes and Glacial lake outburst floods in Nepal. ICIMOD, Patan. ISBN 978-92-9115-193-6. http://lib.icimod.org/record/9419/files/icimod the status of glaciers in the hindu kush-himalayan region [1].pdf.

Kafy, A.A., Rahman, M.S., Hasan, M.M. and Islam, M., 2020. Modelling future land use land cover changes and their impacts on land surface temperatures in Rajshahi, Bangladesh. *Remote Sensing Applications: Society and Environment*, *18*, p.100314. https://doi.org/10.1016/j.rsase.2020.100314.

Kang, S., Xu, Y., You, Q., Flügel, W.A., Pepin, N. and Yao, T., 2010. Review of climate and cryospheric change in the Tibetan Plateau. *Environmental research letters*, *5*(1), p.015101. https://doi.org/10.1088/1748-9326/5/1/015101.

Keshtkar, H., Voigt, W., 2016. A spatiotemporal analysis of landscape change using an integrated Markov chain and cellular automata models. Model. Earth Syst. Environ. 2, 10. https://doi.org/10.1007/s40808-015-0068-4.

Khadka, N., Zhang, G. and Thakuri, S., 2018. Glacial lakes in the Nepal Himalaya: Inventory and decadal dynamics (1977–2017). *Remote Sensing*, *10*(12), p.1913. https://doi.org/10.3390/rs10121913.

Kimura, F. and Shimizu, Y., 1994. Estimation of sensible and latent heat fluxes from soil surface temperature using a linear air-land heat transfer model. *Journal of Applied Meteorology and Climatology*, *33*(4), pp.477-489. DOI: https://doi.org/10.1175/1520-0450(1994)033<0477:EOSALH>2.0.CO;2.

Kothawale, D.R. and Rupa Kumar, K., 2005. On the recent changes in surface temperature trends over India. *Geophysical Research Letters*, *32*(18). https://doi.org/10.1029/2005GL023528.

Liu, J.J., Tang, C., Cheng, Z.L., 2013. The two main mechanisms of glacier lake outburst flood in Tibet, China. Journal of Mountain Science 10 (2), 239-248. https://doi.org/10.1007/s11629-013-2517-8.

Liu, X. and Chen, B., 2000. Climatic warming in the Tibetan Plateau during recent decades. *International Journal of Climatology: A Journal of the Royal Meteorological Society*, *20*(14), pp.1729-1742. https://doi.org/10.1002/1097-0088(20001130)20:14%3C1729::AID-JOC556%3E3.0.CO;2-Y.

Lu, R., Li, D., 1989. Ice-snow-melt water debris flows in the Dongru Longba (Gully) Bomi County, Xizang (Tibet). Journal of Glaciology and Geocryology 2, 148e160 (in Chinese).

Lü, R., Tang, B. and Li, D., 1999. Introduction of debris flow resulted from glacial lakes failed. Debris Flow and Environment in Tibet, Chengdu (China), pp.69-105.

Majeed, U., Rashid, I., Sattar, A., Allen, S., Stoffel, M., Nüsser, M. and Schmidt, S., 2021. Recession of Gya Glacier and the 2014 glacial lake outburst flood in the Trans-Himalayan region of Ladakh, India. *Science of the Total Environment*, *756*, p.144008. https://doi.org/10.1016/j.scitotenv.2020.144008.

Mann, M.E., Bradley, R.S. and Hughes, M.K., 1999. Northern hemisphere temperatures during the past millennium: Inferences, uncertainties, and limitations. *Geophysical research letters*, *26*(6), pp.759-762. https://doi.org/10.1029/1999GL900070.

Maskey, S., Kayastha, R.B. and Kayastha, R., 2020. Glacial lakes outburst floods (GLOFs) modelling of Thulagi and lower Barun glacial lakes of Nepalese Himalaya. *Progress in Disaster Science*, *7*, p.100106. https://doi.org/10.1016/j.pdisas.2020.100106.

Mathew, A., Sreekumar, S., Khandelwal, S., Kaul, N. and Kumar, R., 2016. Prediction of surface temperatures for the assessment of urban heat island effect over Ahmedabad city using linear time series model. *Energy and Buildings*, *128*, pp.605-616. https://doi.org/10.1016/j.enbuild.2016.07.004.

Maurer, J.M., Schaefer, J.M., Russell, J.B., Rupper, S., Wangdi, N., Putnam, A.E. and Young, N., 2020. Seismic observations, numerical modeling, and geomorphic analysis of a glacier lake outburst flood in the Himalayas. Science advances, 6(38), p.eaba3645.

McCarthy, M. P., Best, M. J., & Betts, R. A. (2010). Climate change in cities due to global warming and urban effects. *Geophysical research letters*, *37*(9). https://doi.org/10.1029/2010GL042845.

Mildrexler, D.J., Zhao, M. and Running, S.W., 2011. A global comparison between station air temperatures and MODIS land surface temperatures reveals the cooling role of forests. *Journal of Geophysical Research: Biogeosciences*, *116*(G3). https://doi.org/10.1029/2010JG001486.

Miles, E. S., Steiner, J., Willis, I., Buri, P., Immerzeel, W. W., Chesnokova, A., et al. (2017). Pond dynamics and supraglacial-englacial connectivity on debris-covered Lirung Glacier, Nepal. Front. Earth Sci. 5:69. doi: 10.3389/feart.2017.00069. https://doi.org/10.3389/feart.2017.00069.

Mohanty, L. and Maiti, S., 2021. Probability of glacial lake outburst flooding in the Himalaya. Resources, Environment and Sustainability, 5, p.100031. https://doi.org/10.1016/j.resenv.2021.100031.

Mool, P.K., Bajracharya, S.R., Shrestha, B., Joshi, S.P., Roohi, R., Ashraf, A., Naz, R., Hussain, S.A. and Chaudhry, M.H., 2003. Inventory of glaciers, glacial lakes and the identification of potential glacial lake outburst floods (GLOFs) affected by global warming in the mountains of Himalayan region: Tista Basin, Sikkim Himalaya, India. *Unpublished project report, with database on CD-ROM, prepared for APN and ICIMOD, Kathmandu*, pp.1-136.

Mool, P.K., Maskey, P.R., Koirala, A., Joshi, S.P., Lizong, W., Shrestha, A.B., Eriksson, M., Gurung, B., Pokharel, B., Khanal, N.R. and Panthi, S., 2011. *Glacial lakes and glacial lake outburst floods in Nepal* (No. 98829, pp. 1-109). The World Bank.

Narama, C., Daiyrov, M., Duishonakunov, M., Tadono, T., Sato, H., Kääb, A., Ukita, J. and Abdrakhmatov, K., 2018. Large drainages from short-lived glacial lakes in the Teskey Range, Tien Shan Mountains, Central Asia. *Natural Hazards and Earth System Sciences*, *18*(4), pp.983-995. https://doi.org/10.5194/nhess-18-983-2018.

Pandey, P., Chauhan, P., Ray, P.K. C., Sharma, P., Chattoraj, S.L., Sharma, Richa., Nainwal, H.C., Ali,, S.N., Singh, R., 2020. Glacial lakes of Uttarakhand. Published by Indian Institute of Remote Sensing, Indian Space Research Organisation, Dehradun.

Petrakov, D.A., Tutubalina, O.V., Aleinikov, A.A., Chernomorets, S.S., Evans, S.G., Kidyaeva, V.M., Krylenko, I.N., Norin, S.V., Shakhmina, M.S. and Seynova, I.B., 2012. Monitoring of Bashkara Glacier lakes (Central Caucasus, Russia) and modelling of their potential outburst. *Natural Hazards*, *61*(3), pp.1293-1316. https://doi.org/10.1007/s11069-011-9983-5.

Petrakov, D.A., Chernomorets, S.S., Viskhadzhieva, K.S., Dokukin, M.D., Savernyuk, E.A., Petrov, M.A., Erokhin, S.A., Tutubalina, O.V., Glazyrin, G.E., Shpuntova, A.M. and Stoffel, M., 2020. Putting the poorly documented 1998 GLOF disaster in Shakhimardan River valley (Alay Range, Kyrgyzstan/Uzbekistan) into perspective. *Science of The Total Environment*, *724*, p.138287. https://doi.org/10.1016/j.scitotenv.2020.138287.

Pu, R., Gong, P., Michishita, R. and Sasagawa, T., 2006. Assessment of multi-resolution and multi-sensor data for urban surface temperature retrieval. Remote Sensing of Environment, 104(2), pp.211-225. https://doi.org/10.1016/j.rse.2005.09.022.

Rai, S.C., 2005. An Overview of Glaciers, Glacier Retreat and Subsequent Impacts in Nepal, India and China. WWF Nepal Program, Nepal.

Reynolds, J. M. (2000). "On the formation of supraglacial lakes on Debris-Covered Glaciers," in Proceedings of a workshop Debris-Covered Glaciers (Seattle, WA), 153–164.

Reynolds, J.M., 1992. The identification and mitigation of glacier-related hazards: examples from the Cordillera Blanca, Peru. In: McCall, G.J.H., Laming, D.C.J., Scott, S. (Eds.), Geo-hazards. Chapman and Hall, London. https://doi.org/10.1007/978-94-009-0381-4_13.

Riaz, S., A. Ali, and M.N. Baig. 2014. Increasing risk of glacial lake outburst floods as a consequence of climate change in the Himalayan region. Journal of Disaster Risk Studies 6 (1): 1–7. doi:10.4102/jamba.v6i1.110. http://hdl.handle.net/10394/13920.

Rudoy, A.N., 2002. Glacier-dammed lakes and geological work of glacial superfloods in the Late Pleistocene, Southern Siberia, Altai Mountains. Quaternary International 87, 119e140. https://doi.org/10.1016/S1040-6182(01)00066-0.

Running, S.W., Justice, C.O., Salomonson, V., Hall, D., Barker, J., Kaufmann, Y.J., Strahler, A.H., Huete, A.R., Muller, J.P., Vanderbilt, V. and Wan, Z.M., 1994. Terrestrial remote sensing science and algorithms planned for EOS/MODIS. *International journal of remote sensing*, *15*(17), pp.3587-3620. https://doi.org/10.1080/01431169408954346.

Sah, M., Philip, G., Mool, P.K., Bajracharya, S. and Shrestha, B., 2005. Inventory of glaciers and glacial lakes and the identification of potential glacial lake outburst floods (GLOFs) affected by global warming in the mountains of Himalayan region: Uttaranchal Himalaya, India; Unpublished Project Report, ICIMOD, Kathmandu.

Sakai, A., Chikita, K., and Yamada, T. (2000). Expansion of a moraine-dammed glacial lake, Tsho Rolpa, in Rolwaling Himal, Nepal Himalaya. Limnol. Oceanogr. 45, 1401–1408. doi: 10.4319/lo.2000.45.6.1401. https://doi.org/10.4319/lo.2000.45.6.1401.

Schmidt, S., Nüsser, M., Baghel, R. and Dame, J., 2020. Cryosphere hazards in Ladakh: the 2014 Gya glacial lake outburst flood and its implications for risk assessment. *Natural Hazards*, *104*(3), pp.2071-2095.

Schmandt, B., Aster, R.C., Scherler, D., Tsai, V.C. and Karlstrom, K., 2013. Multiple fluvial processes detected by riverside seismic and infrasound monitoring of a controlled flood in the Grand Canyon. *Geophysical Research Letters*, *40*(18), pp.4858-4863. https://doi.org/10.1007/s11069-020-04262-8.

Seleshi, Y. and Zanke, U., 2004. Recent changes in rainfall and rainy days in Ethiopia. *International Journal of Climatology: A Journal of the Royal Meteorological Society*, *24*(8), pp.973-983. https://doi.org/10.1002/joc.1052.

Seleshi, Y. and Zanke, U., 2004. Recent changes in rainfall and rainy days in Ethiopia. International Journal of Climatology: A Journal of the Royal Meteorological Society, 24(8), pp.973-983. https://doi.org/10.1002/joc.1052.

Shi-Jin, W. and Lan-Yue, Z., 2019. Integrated impacts of climate change on glacier tourism. *Advances in Climate Change Research*, *10*(2), pp.71-79. https://doi.org/10.1016/j.accre.2019.06.006.

Shrestha, A.B. and Devkota, L.P., 2010. *Climate change in the Eastern Himalayas: observed trends and model projections*. International Centre for Integrated Mountain Development (ICIMOD).

Shrestha, A.B., Wake, C.P., Mayewski, P.A. and Dibb, J.E., 1999. Maximum temperature trends in the Himalaya and its vicinity: an analysis based on temperature records from Nepal for the period 1971–94. *Journal of climate*, *12*(9), pp.2775-2786. https://doi.org/10.1175/1520-0442(1999)012%3C2775:MTTITH%3E2.0.CO;2.

Shukla A, Garg PK and Srivastava S (2018) Evolution of Glacial and High-Altitude lakes in the Sikkim, Eastern Himalaya Over the Past Four Decades (1975-2017). Front. Environ. Sci. 6:81. doi: 10.3389/fenvs.2018.00081. https://doi.org/10.3389/fenvs.2018.00081.

Shukla, T., Mehta, M., Jaiswal, M.K., Srivastava, P., Dobhal, D.P., Nainwal, H.C. and Singh, A.K., 2018. Late Quaternary glaciation history of monsoon-dominated Dingad basin, central Himalaya, India. Quaternary Science Reviews, 181, pp.43-64. https://doi.org/10.1016/j.quascirev.2017.11.032.

Streutker, D.R., 2002. A remote sensing study of the urban heat island of Houston, Texas. International Journal of Remote Sensing, 23(13), pp.2595-2608. https://doi.org/10.1080/01431160110115023.

Tabari, H., Taye, M.T. and Willems, P., 2015. Statistical assessment of precipitation trends in the upper Blue Nile River basin. *Stochastic environmental research and risk assessment*, *29*(7), pp.1751-1761. https://doi.org/10.1007/s00477-015-1046-0.

Taloor, A.K., Kothyari, G.C., Manhas, D.S., Bisht, H., Mehta, P., Sharma, M., Mahajan, S., Roy, S., Singh, A.K. and Ali, S., 2021. Spatio-temporal changes in the Machoi glacier Zanskar Himalaya India using geospatial technology. *Quaternary Science Advances*, p.100031. https://doi.org/10.1016/j.qsa.2021.100031.

Thompson, S., Benn, D. I., Mertes, J., and Luckman, A. (2016). Stagnation and mass loss on a Himalayan debris-covered glacier: processes, patterns and rates. J. Glaciol. 62, 467–485. doi: 10.1017/jog.2016.37. https://doi.org/10.1017/jog.2016.37.

United Nations, 2010. World urbanization prospects: The 2009 revision population database. http://esa.un.org/unpd/wup/index.htm.

United Nations, Department of Economic and Social Affairs, Population Division (2019). World Urbanization Prospects: The 2018 Revision (ST/ESA/SER.A/420). New York: United Nations.

United Nations, Department of Economic, Social Affairs, P.D., 2018. World Urbanization Prospects: the 2018 Revision.

Urban, M., Eberle, J., Hüttich, C., Schmullius, C. and Herold, M., 2013. Comparison of satellite-derived land surface temperature and air temperature from meteorological stations on the pan-Arctic Scale. *Remote Sensing*, *5*(5), pp.2348-2367. https://doi.org/10.3390/rs5052348.

USGS, *Landsat 8 Data Users Handbook*, USGS, Reston, VA, USA, 2016.

Vancutsem, C., Ceccato, P., Dinku, T. and Connor, S.J., 2010. Evaluation of MODIS land surface temperature data to estimate air temperature in different ecosystems over Africa. *Remote Sensing of Environment*, *114*(2), pp.449-465. https://doi.org/10.1016/j.rse.2009.10.002.

Voogt, J.A. and Oke, T.R., 2003. Thermal remote sensing of urban climates. Remote sensing of environment, 86(3), pp.370-384. https://doi.org/10.1016/S0034-4257(03)00079-8.

Walder, J.S., Costa, J.E., 1996. Outburst floods from glacier-dammed lakes: the effect of mode of lake drainage on flood magnitude. Earth Surface Processes and Landforms 21 (8), 701e723. https://doi.org/10.1002/(SICI)1096-9837(199608)21:8%3C701::AID-ESP615%3E3.0.CO;2-2.

Walder, J.S., Driedger, D.L., 1995. Frequent outburst floods from south Tahoma glacier, Mount Rainier, USA: relation to debris flow, meteorological origin and implications for subglacial hydrology. Journal of Glaciology 41 (137), 1e10. https://doi.org/10.3189/S0022143000017718.

Wang, S.J. and Zhou, L.Y., 2019. Integrated impacts of climate change on glacier tourism. Adv Clim Chang Res 10 (2): 71–79. https://doi.org/10.1016/j.accre.2019.06.006.

Warren, C. R., and Kirkbride, M. P. (1998). Temperature and bathymetry of ice-contact lakes in Mount Cook National Park, New Zealand. N. Z. J. Geol. Geophys. 41, 133–143. doi: 10.1080/00288306.1998.9514797. https://doi.org/10.1080/00288306.1998.9514797.

Weng, Q. and Fu, P., 2014. Modeling diurnal land temperature cycles over Los Angeles using downscaled GOES imagery. *ISPRS Journal of Photogrammetry and Remote Sensing*, *97*, pp.78-88. https://doi.org/10.1016/j.isprsjprs.2014.08.009.

Westoby, M. J., Glasser, N. F., Brasington, J., Hambrey, M. J., Quincey, D. J., and Reynolds, J. M. (2014). Modelling outburst floods from moraine-dammed glacial lakes. Earth Sci. Rev. 134, 137–159. doi: 10.1016/j.earscirev.2014.03.009. https://doi.org/10.1016/j.earscirev.2014.03.009.

Worni R, Stoffel M, Huggel C, Volz C, Casteller A, Luckman B (2012) Analysis and dynamic modeling of a moraine failure and glacier lake outburst flood at Ventisquero Negro, Patagonian Andes (Argentina). J Hydrol 444–445:134–145. https://doi.org/10.1016/j.jhydrol.2012.04.013.

Worni, R., Huggel, C. and Stoffel, M., 2013. Glacial lakes in the Indian Himalayas—From an area-wide glacial lake inventory to on-site and modeling-based risk assessment of critical glacial lakes. *Science of the Total Environment*, *468*, pp.S71-S84. https://doi.org/10.1016/j.scitotenv.2012.11.043.

Xiao, J., Shen, Y., Ge, J., Tateishi, R., Tang, C., Liang, Y. and Huang, Z., 2006. Evaluating urban expansion and land use change in Shijiazhuang, China, by using GIS and remote sensing. Landscape and urban planning, 75(1-2), pp.69-80. https://doi.org/10.1016/j.landurbplan.2004.12.005.

Yao, T., Thompson, L., Yang, W., Yu, W., Gao, Y., Guo, X., Yang, X., Duan, K., Zhao, H., Xu, B. and Pu, J., 2012a. Different glacier status with atmospheric circulations in Tibetan Plateau and surroundings. *Nature climate change*, *2*(9), pp.663-667. https://doi.org/10.1038/nclimate1580.

Yao, T., Thompson, L.G., Mosbrugger, V., Zhang, F., Ma, Y., Luo, T., Xu, B., Yang, X., Joswiak, D.R., Wang, W. and Joswiak, M.E., 2012b. Third pole environment (TPE). *Environmental Development*, *3*, pp.52-64. https://doi.org/10.1016/j.envdev.2012.04.002.

Yuan, F. and Bauer, M.E., 2007. Comparison of impervious surface area and normalized difference vegetation index as indicators of surface urban heat island effects in Landsat imagery. Remote Sensing of environment, 106(3), pp.375-386. https://doi.org/10.1016/j.rse.2006.09.003.

Yue, S., Pilon, P. and Cavadias, G., 2002. Power of the Mann–Kendall and Spearman's rho tests for detecting monotonic trends in hydrological series. *Journal of hydrology*, *259*(1-4), pp.254-271. https://doi.org/10.1016/S0022-1694(01)00594-7.

Yuen, B., Kong, L., 2009. Climate change and urban planning in Southeast Asia.SAPIENS 2, 2-3. http://journals.openedition.org/sapiens/881.

Zhang, Y. and Sun, L., 2019. Spatial-temporal impacts of urban land use land cover on land surface temperature: Case studies of two Canadian urban areas. *International Journal of Applied Earth Observation and Geoinformation*, *75*, pp.171-181. https://doi.org/10.1016/j.jag.2018.10.005.

Ethical Statement and Conflict of Interest

We declare that all ethical practices have been followed in relation to the development, writing, and publication of the article.

Authors declare no conflict of interest.